TU Delft
Delft University of Technology

Literature review

The Effect of Groynes on Rivers

Mohamed F. M. Yossef

Delft Cluster

Dioc "Water"

The Effect of Groynes on Rivers

Literature review

Mohamed F. M. Yossef

Delft University of Technology
Faculty of Civil Engineering and Geosciences
Section of Hydraulic Engineering
e-mail: M.F.Y.Yossef@citg.tudelft.nl

Delft Cluster project no. 03.03.04

23 August, 2002

Delft University of Technology
Faculty of Civil Engineering and Geosciences
Section of Hydraulic Engineering

23 August, 2002

Foreword

The following report is a literature review study carried out to acquire the background knowledge, and the state of the art concerning the effect of groynes on rivers, as part of the author's Ph.D. study. This study is carried out within the framework of DIOC Water, theme 1.3 (Intermediate-scale morphological developments in rivers due to human interventions) and Delft Cluster, theme 3 (Coasts and Rivers).

Abstract

Groynes are structures constructed at an angle to the flow in order to deflect the flowing water away from critical zones. They are made of stone, gravel, rock, earth, or piles, beginning at the riverbank with a root and ending at the regulation line with a head. They serve to maintain a desirable channel for the purpose of flood control, improved navigation and erosion control. In the River Rhine, which is considered the backbone of North-western European waterways network, the primary objective of groynes is to provide a fairway of sufficient depth and width. For example the River Waal, the most important branch of the Rhine River in the Netherlands is regulated by around 500 groyne.

Within the framework of the research project "*Space for the Rhine Branches*" several measures have been devised to achieve a decrease of the water levels at peak discharges, one of those measures, is lowering of the existing groynes. The rationale behind this proposal is that; due to large-scale erosion of the low-water bed through the past decades, the groynes are now higher than necessary for keeping the main channel at depth. Lowering the groynes along certain reaches of the river would result in a reduction of the effective roughness during high water conditions thus, increasing the river's flood conveyance capacity.

If the groynes are lowered, however, the balance of hydrodynamic forces acting on the groyne-fields will change, and there will be a large-scale morphological impact. To identify this impact, a thorough understanding to the effect of groynes on the morphology of the river is necessary. The sediment exchange between the groyne-fields and the main channel needs to be more comprehensible.

The purpose of this report is to acquire the background knowledge required to study the effect of groynes on a river. The characteristics of the existing groyne-fields along the Waal River are presented. The hydrodynamic and morphological impact of groynes on a river is described. Moreover, because navigation plays an important role in the interaction between the groyne fields and the main channel, the navigation induced water motion and its effect on the flow in groyne-fields is described. Finally, a review of some prediction attempts to the interaction between the groyne-fields and the main channel is presented.

Table of Contents

1. Introduction

1.1. Background ---- 1
1.2. Objective ---- 2
1.3. Scale of the problem ---- 2
1.4. Outlines of this report ---- 3

2. Characteristics of Groynes

2.1. General ---- 4
2.2. Transverse structures – groynes ---- 4
2.2.1. Types of groynes ---- 4
2.2.2. Design Considerations for Groynes ---- 5
2.3. Groynes in the Netherlands ---- 7
2.3.1. Historical background ---- 7
2.3.2. Characteristics of the groyne-fields along the Waal River ---- 9

3. The Effect of Groynes on a River

3.1. Flow near groynes ---- 12
3.1.1. Flow near a single groyne ---- 12
3.1.2. Flow pattern in groyne-fields ---- 14
3.1.3. Submerged groynes ---- 17
3.2. Morphological Effect of Groynes on a River ---- 18
3.2.1. General ---- 18
3.2.2. Bed Degradation Caused By Long Constriction ---- 18
3.2.3. Bed Degradation Caused By Series of Groynes ---- 20
3.2.4. Local Scour Near Groynes ---- 21

4. Hydraulic Disturbances Caused by Navigation

4.1. Navigation induced water motion ---- 25
4.1.1. Water movement around a ship ---- 25
4.1.2. Return current and water level depression ---- 26
4.1.3. Ship waves ---- 28
4.2. Effect of navigation on the flow in a groyne-field ---- 28

5. Morphological Interaction between the Groyne-Fields and the Main Channel

5.1. General ---- 32
5.2. Estimation of erosion from groyne-fields ---- 32
5.2.1. Field studies ---- 33
5.2.2. Analytical approach ---- 35
5.3. Effect of changing the existing groynes geometry ---- 39
5.3.1. Lowering the groynes ---- 39
5.3.2. Lengthening or shortening of groynes ---- 40
5.3.3. Decreasing the groynes spacing ---- 40

References ***41***

Appendix I – Conceptual Model ***44***

Appendix II – The model of Sieben & Douben ***47***

1. INTRODUCTION

1.1. BACKGROUND

In 1992, the World Wildlife Found published a report named 'Living Rivers'. This plan has the objective to recover the natural river landscape that will lead to a return of river characteristic plants and animals. Next to this plan, many initiatives and plans from different points of view, like navigation, nature and landscape have been published. However, safety should always have the first priority and not to be put aside for nature development. For example, the construction of flood plain forests will lead to an increased roughness of the river and to higher water levels upstream. It is possible to find engineering compensation by e.g. lowering the groynes. In this case, nature and safety would go hand in hand. However, the impact on the morphology in this case is unclear, which means navigation might be in danger. This example emphasises that the river is a coherent system, in which every engineering measure has implications on all the functions of the riverine area. Consequently, the decision to execute any of the measures must be supported by good arguments. In this way actors and stakeholders can be informed on the advantages and disadvantages of the measure and decide if the measure is socially desirable.

Within the framework of the research project "*Ruimte voor Rijntakken*" (in English: "*Space for the Rhine Branches*") several measures have been devised to achieve a decrease of the water levels at peak discharges, by means of enlarging river space. A wide range of fourteen measures is mentioned in detail in the '*Landscape Planning River Rhine*' (*LPR*) report, (see Figure 1-1). One of those measures, is lowering of the existing groynes, say by 2 m is proposed.

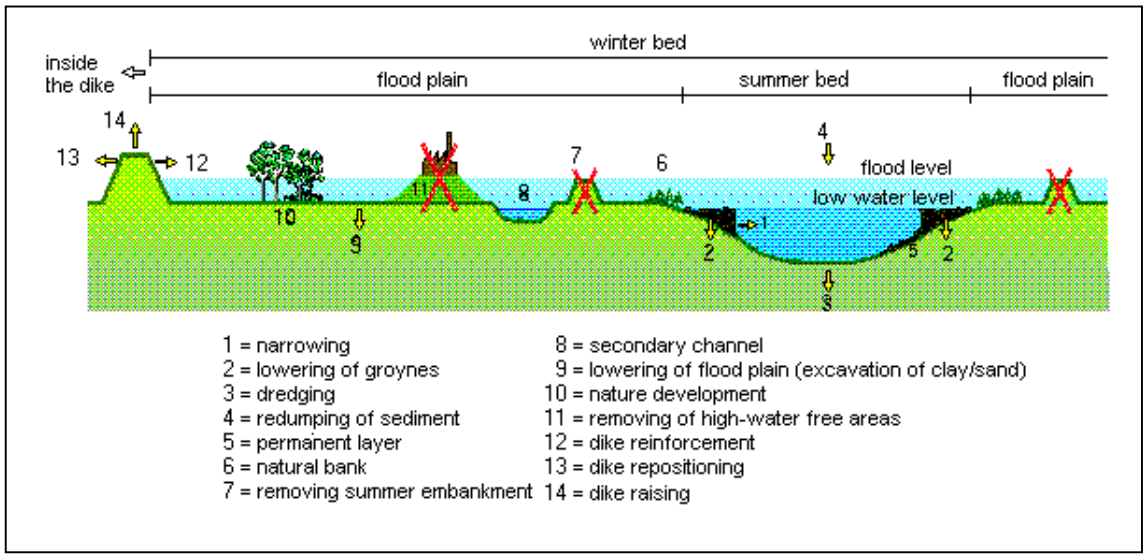

Figure 1-1 River engineering measures as proposed in *LPR* report

The rationale behind this proposal is that; due to large-scale erosion of the low-water bed through the past decades, the groynes that were constructed between 1860 and 1920 are higher than strictly necessary for keeping the main channel at depth. Lowering the groynes along certain reaches of the river, an activity requires a huge investment, would result in a reduction of the effective roughness during high water conditions. Thus, increasing the river's flood conveyance capacity. This increased flood capacity would help restoring some of the riverine nature, which would in turn, increase the effective roughness. This is important in the light of the policy objective to accommodate higher flood discharges without raising the dikes.

1.2. OBJECTIVE

If the groynes are lowered, however, the balance of hydrodynamic forces acting on the groyne-fields will change, and there will be a large-scale morphological impact. This may involve for example; tilting of the entire river, similar to the effect of the normalisation works in the first half of the previous century. It may also involve the necessity of dredging or other maintenance measures, so as to ensure desired navigable depth.

To carry on with such a plan, a thorough understanding to the effect of groynes on the morphology of the river is necessary. The sediment exchange between the groyne-fields and the main channel needs to be more comprehensible.

1.3. SCALE OF THE PROBLEM

Before going into the details of the problem, it is wise to classify the scale of the problem. Following the classification of de Vriend (1999), the morphological process of a river could be represented by a series of scale levels. Assuming that to some extent these scale levels can be considered separately, they form a sort of cascade (Figure 1-2), in which, the micro-scale level represents the small-scale bedforms, e.g. ripples and dunes. The meso-scale level is that of alternate bars and cross sectional-profile evolution. The macro-scale level is that of meander formation, up to longitudinal profile evolution of river reaches, e.g. in response to training works. Channel pattern formation at the scale of the river basin constitutes the mega-scale.

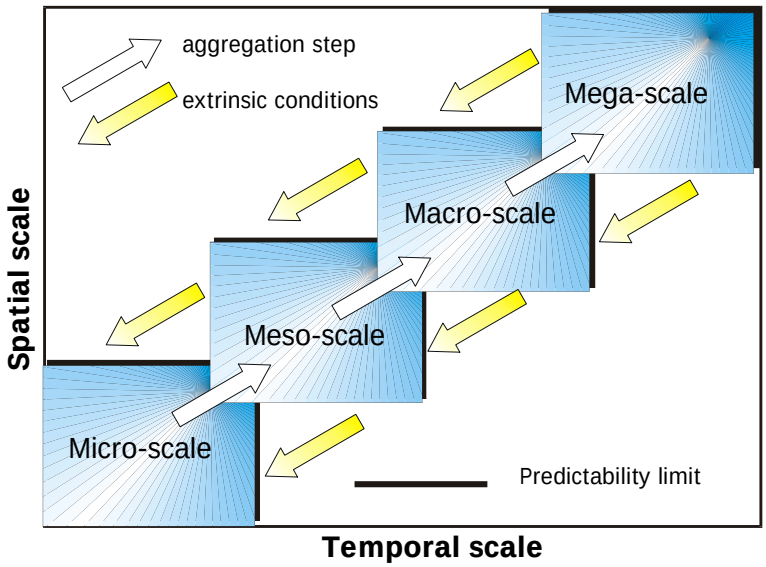

Figure 1-2 Scale cascade of morphological process according to de Vriend (1999)

In our case, we will adopt a rather simplified classification from that of de Vriend (1999). It consists of two levels, a small-scale level, and a large-scale level. The small scale is to some extent a combination between the micro and meso-scales of de Vriend. The large scale is equivalent to the macro-scale while the mega-scale is beyond the scope of this study. The small-scale analysis will be devoted to study in detail the local behaviour of a single/few groyne-fields under the effect of the different hydrodynamic forcings, “spatial distinction”, for a period which is relatively short “temporal distinction”. In the large-scale analysis, the impact on the whole river system will be considered. The results from the small-scale analysis will then be aggregated to form some kind of a forcing function to the large-scale stage. This function is supposed to be representative of the the small-scale phenomena. An example is presented in Appendix I for a conceptual model for the interaction between the groyne-fields and the main channel.

The hydrodynamic forcing that governs the interaction between the groyne-fields and the main channel is the resultant of two components. The first is the effect of navigation, which is a factor that cannot be overlooked in a river like the River Rhine that is considered the backbone of the North west European waterways network. The other is the current induced water motion. On the one hand, the groyne-fields are filled with sediment during times of high discharge. On the other hand, the navigation induced water motion is held responsible for eroding the groyne-field beaches; this effect is largest during low discharges. For an overview on the different parameters that are affecting the interaction between the groyne-fields and the main channel, see Figure 1-3.

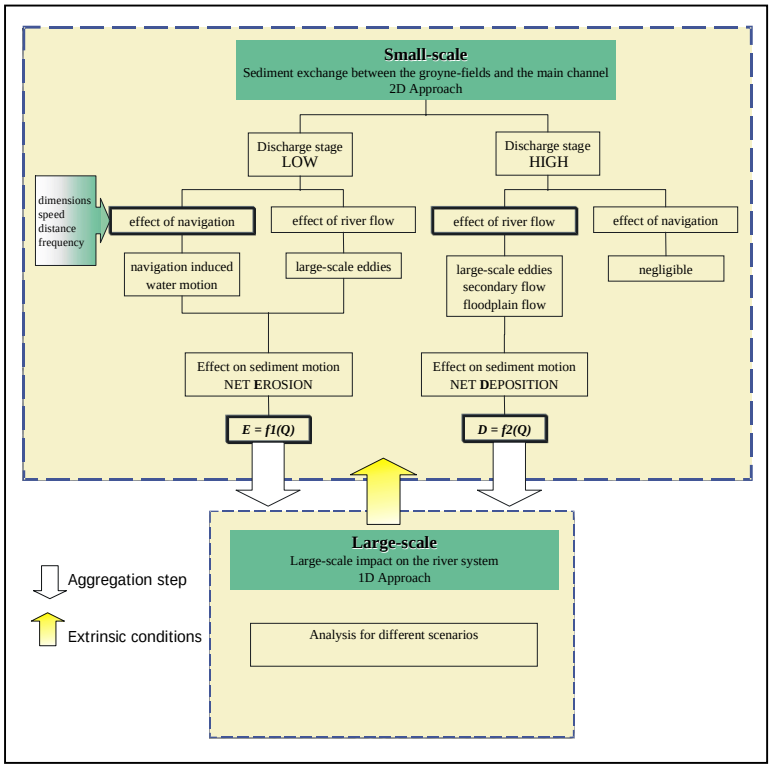

Figure 1-3 Overview on the parameters that affect the interaction between the groyne-fields and the main channel

1.4. OUTLINES OF THIS REPORT

The aim of this report is to acquire the background knowledge required to study the morphological interaction between the groyne-fields and the main channel. Chapter 2 describes aspects and consideration for groynes construction, presenting the different types of groynes. Furthermore, the characteristics of the groyne-fields along the Waal River are presented. Chapter 3 describes the hydrodynamic and morphological impact of groynes on a river. In Chapter 4, navigation induced water motion and its effect on the flow in groyne-fields is described. In chapter 5, a review of some prediction attempts to the interaction between the groyne-fields and the main channel is presented.

2. CHARACTERISTICS OF GROYNES

2.1. GENERAL

River training is the stabilisation of the channel in order to maintain the desired cross section and alignment. The practice of training a river dates back to the sixteenth century where the Yellow River in China was trained by building embankments along its banks so that the flow would be confined to a single deep channel, which would transport the sediment load to the sea. Modern river training practice, however, started in Europe in the nineteenth century, driven by the demands of the industrial revolution for the purpose of maintaining sufficient channel depth and a better course for navigation.

In general, the objectives of river training may be summarised as:

- to increase the safety against flooding by accommodating the flood flow
- to improve the efficiency of the sediment transport
- to minimise bank erosion by stabilising the course of flow
- to direct the flow to a desired river stretch
- to reduce the probability of ice jamming
- and in most of the cases the primary objective of river training is to improve navigation by maintaining channel depth

Natural processes and human interference may disturb the equilibrium between the sediment load contributed to the channel and the transport capacity of the flow. Seasonal variations in the flow, dredging of the river, construction of a reservoir, and deforestation in the catchment area are all examples of causes of disturbance. Training structures are then necessary in order to protect the channel against the changes that occur due to this disturbance. They could be classified into:

i. Bed fixation and bottom vanes
ii. Longitudinal structures
iii. Transverse structures

In this report, the focus will be only on the groynes as a transverse structure. For a complete review of all river-regulating systems, see Przedwojski et al. (1995).

2.2. TRANSVERSE STRUCTURES – GROYNES

Groynes are structures constructed at an angle to the flow in order to deflect the flowing water away from critical zones. They are made of stone, gravel, rock, earth, or piles, beginning at the riverbank with a root and ending at the regulation line with a head. They serve to maintain a desirable channel for the purpose of flood control, improved navigation and erosion control.

2.2.1. Types of groynes

Various types of groynes can be distinguished according to their construction, action on stream flow and appearance. Beckstead (1975), (*as reported by Przedwojski et al. 1995*) considers the following, necessary for a full description of groynes:

i. Classification according to the method and materials of construction:
   Groynes may be permeable allowing the water to flow through at reduced velocities or impermeable blocking and deflecting the current. Permeable groynes are fabricated from piles; bamboo or timbers whereas impermeable groynes also called solid groynes, are constructed using rock, gravel, or gabions.

ii. Classification according to submergence:
Groynes may be designed either as submerged or as non-submerged. Which of the two types will be used is dictated by the design conditions. Usually impermeable groynes are designed to be non-submerged since flow over the top of solid groynes may cause severe erosion along the shanks. For submerged conditions, on the other hand, permeable groynes may be designed owing to the fact that they disturb the flow much less than solid groynes.

iii. Classification according to the action on the stream flow:
Groynes may be classified as attracting, deflecting or repelling groynes. Attracting groynes point downstream, they serve to attract the stream flow towards themselves and do not repel the flow towards the opposite bank. Deflecting groynes are generally short ones and used for local protection. They serve to change the direction of flow without repelling it. Repelling groynes point upstream. They serve to repel the flow away from themselves.

iv. Classification according to their appearance in plan:
Groynes may be built with different planview shapes. Examples are straight groynes, T-head, L-head, hockey shaped, inverted hockey shaped groynes, straight groynes with pier head, wing, or tail groynes.

2.2.2. Design Considerations for Groynes

The most important considerations involved in groyne design are planview shape, length of the groynes, spacing between groynes, orientation to the flow, crest elevation and slope, cross-section, construction materials and scour; Alvarez (1989), Richardson et al. (1975), and Przedwojski et al. (1995).

i. Planview shape:
Of the above mentioned types of groynes according to their appearance in planview, the straight groyne is set at an angle from the bank and has a rounded head to provide extra volume and area for scour protection at the outer end. The T-head groyne is normally set at a right angle from the bank and it has a straight shank with a rectangular guide vane at the outer end. L-head, wing or tail groynes have larger sediment deposits between groynes, less scour at their head, provide greater protection to the banks and are more effective in channelization for navigation when the length closes 45 to 65 percent of the gap between groynes. Hockey-shaped groynes have scour holes that are more extensive in area than the T-head groynes.

ii. Length of the groynes:
Groyne length depends on the location, purpose, spacing, and economics of construction. The total length of the groyne includes the anchoring length, which remains embedded in the bank, and the working length, which stays in the flow. The length can be established by determining the channel width and depth desired. The working length is usually kept between the lower and upper limits of the mean depth and a quarter of the mean width of the free surface respectively. The anchoring length on the other hand is recommended to be less than a quarter of the working length.

iii. Spacing between groynes:
The spacing between groynes is measured at the riverbank between their starting points. It is related to river width, groyne length, velocity of flow, angle to the bank, orientation to the flow, bank curvature, and purpose. However, it is often expressed as a multiple of the groyne length. Richardson (1975) recommends a spacing of 1.5 to 6 times the upstream projected groyne length into the flow. In order to obtain a well defined deep channel navigation, to keep a spacing of 1.5 to 2 times the groyne length is recommended, whereas for bank protection the ratio of spacing to groyne length is less and distances from 2 to 6 times the groyne length are generally used, although there exists successful

examples of bank protection with short groynes spaced apart 10 to 100 times their length where the banks are protected with riprap or vegetation. If the spacing between groynes is too long, a meander loop may form between groynes. Long and far apart spaced groynes may contract the flow resulting in channel degradation and bank erosion, and cause a hindrance to navigation. If the groynes are spaced too close together on the other hand, construction costs will be higher and the system would work less efficiently without making best use of each individual groyne.

iv. Orientation of the groynes:

Groynes may be oriented perpendicular to the flow or be inclined either upstream or downstream. Each orientation affects the stream in a different way and results in different deposition of sediment in the vicinity of the groyne. A groyne pointing downstream is an attracting groyne, which attracts the stream flow towards itself. Repelling groynes, which repel the flow away, and deflecting groynes, which deflect the flow away from the bank, point upstream.

A groyne that is oriented upstream causes more deposition than a perpendicular one at the downstream bank and also at the area upstream where a reverse eddy is formed and causes suspended load to settle. The amount of deposition between groynes is maximised in case of upstream inclination due to their ability to protect bank areas upstream and downstream of themselves. Therefore, groynes of this kind are best suited for bank protection and sedimentation purposes. Groynes that are perpendicular to the flow have protection over a smaller area. Downstream facing groynes are not suitable for bank protection purposes due to their attracting effect on the flow. The flow towards the root of the downstream groyne threatens the surrounding bank area as well as the groyne itself. For the purpose of maintaining a deep channel to improve navigation on the other hand, best performance is obtained by perpendicular or downstream pointed groynes.

v. Crest elevation and slope:

The crest elevation of groynes depends on the purpose and possible problems due to overbank flow and ice. For bank protection, the crest should be at least as high as the bank. To avoid ice overtopping the crest elevation should be higher than the expected levels of ice. Crests may be either level or sloping downwards from the bank towards the end of the groyne. For bank protection, sloping-crested groynes are recommended by Alvarez (1989) with a slope of 0.1 to 0.25 due to their advantages of reducing scour at the groyne end, less material needed for construction, faster deposits of sediment between groynes. For navigation channel control, level crested groynes work best normal to the flow or angled downstream, whereas, sloping crested groynes work best normal or angled upstream, Richardson (1975).

vi. Cross-section of the groynes:

The crest widths range from 1to 6m and side slopes from 1:1.25 to 1:5. The minimum crest width of 1m is controlled by the equipment placing the groynes and wider crests make placing easier.

vii. Construction materials:

Examples of the wide range of materials used for the construction of groynes are timber piles, tree trunks or branches, rock, soil gravel, sandbags, riprap, prefabricated concrete elements, steel and wire, etc.

viii. Scour:

The expected scour depth should be taken into consideration in the determination of the base depth of the groynes.

2.3. GROYNES IN THE NETHERLANDS

2.3.1. Historical background

The first major hydraulic engineering works since the Roman era were undertaken at the Rhine bifurcation in the early 1700s. Until then, channel correction had been carried out and groynes, dams, and revetments built, but they served only local proposes such as the protection of dike sections. At the end of the 17th century, the Waal carried by far the greatest part of the Rhine discharge, probably over 95%. Water supply to the Nederrijn and the IJssel was so small that navigation became difficult.

Around 1775, the bifurcation of the Nederrijn and the IJssel was reconstructed by digging a new channel in the upper part of the IJssel. Since then, the IJssel received about one third of the discharge of the Pannerdensch Canal which in turn received about one third of the total Rhine discharge. The Waal carried the remaining two thirds of the flow. Stabilisation of the situation was achieved by moles, constructed under the supervision of Brunings who was one of the first engineers to carryout accurate flow measurements in the river. Until the 1960s, the riverbed of the Oude Rijn continued to function as a spillway for excess water, causing numerous floods in the region, see van Urk & Smit (1989).

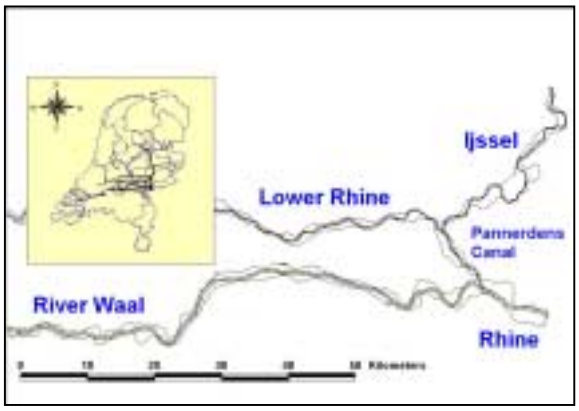

Figure 2-1 Rhine branches – key map

The works at the bifurcations improved water distribution between the Rhine branches, but floods continued to be hazardous. As administrative boards or water authorities with responsibility for integrated river engineering did not exist until the 19th century, individual landowners built bank revetments and groynes to protect their land from erosion and to increase sedimentation. However, the irregular array of groynes and the presence of many sandbars in the channel, not only impeded flow but also led to the formation of ice dams. A formal ban on the irregular construction of groynes proposed by the States of Gelderland in 1602 and finally adopted in 1715, but it had little effect because of the lack of supervision.

In 1809 and 1820, large areas were inundated and in 1821 a government committee was appointed to make proposals for the solution of the problem. In 1825, the committee completed its report, which was published in 1827. Meanwhile, prominent engineers such as Blanken, Goudriaan, and Krayenhoff had published their different views on the best solution. Their recommendations varied from the creation of new spillways by the partial removal of dykes, to the building of sluices, and to the construction of a totally new canal from the entry of the Rhine in the Netherlands to the IJssel, van Urk & Smit (1989). These drastic plans were never carried out. The solution that finally adopted was outlined in a report submitted by inspectors Ferrand and van der Kun of the newly formed Rijkswaterstaat (RWS). It proposed the removal of the sandbars and the constriction of the river's channels to accelerate flow.

As stated before, the channel constriction was the solution finally adopted to increase the discharge capacity of the Lower Rhine. The method of channelization can best be demonstrated in a series of maps for a stretch of the river that was relatively unaffected before work started. Because the wider River Waal has a stronger tendency to form multiple channels than the much narrower, strongly meandering River IJssel, the effect of channel constriction on the Waal was greater. The various operations carried out to transform the unregulated River Waal into a single constricted channel are shown in Figure 2-2, and Figure 2-3.

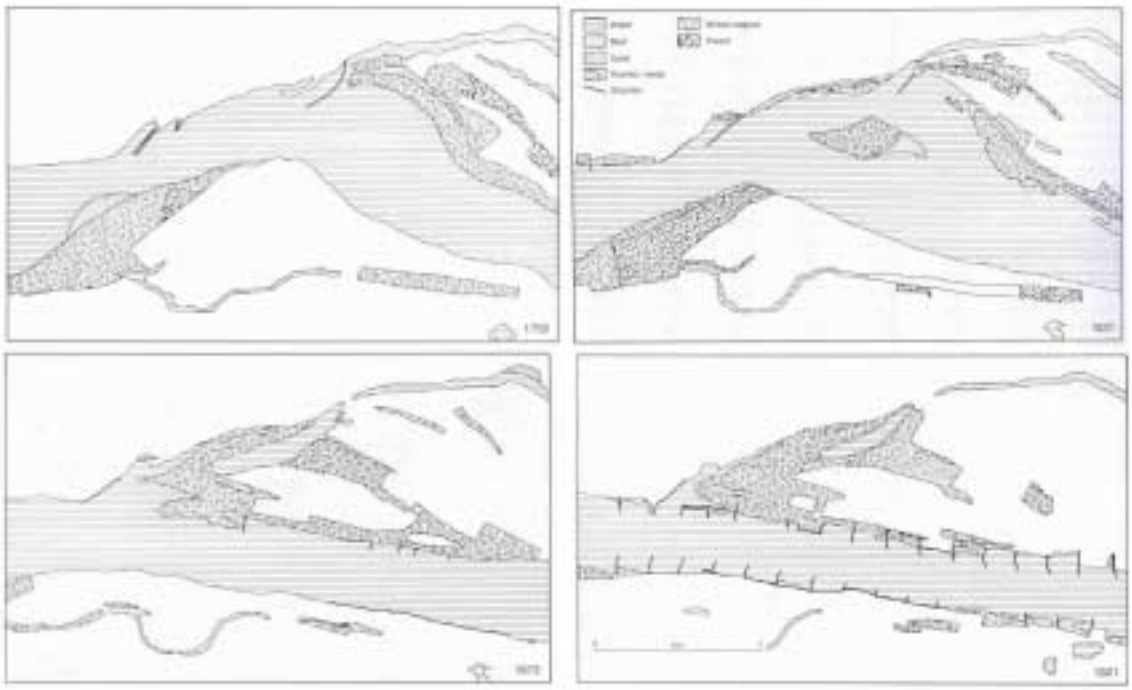

Figure 2-2 The Waal River near Km 899-901 showing the channel changes over period of about 200 years , source: van Urk & Smit (1989).

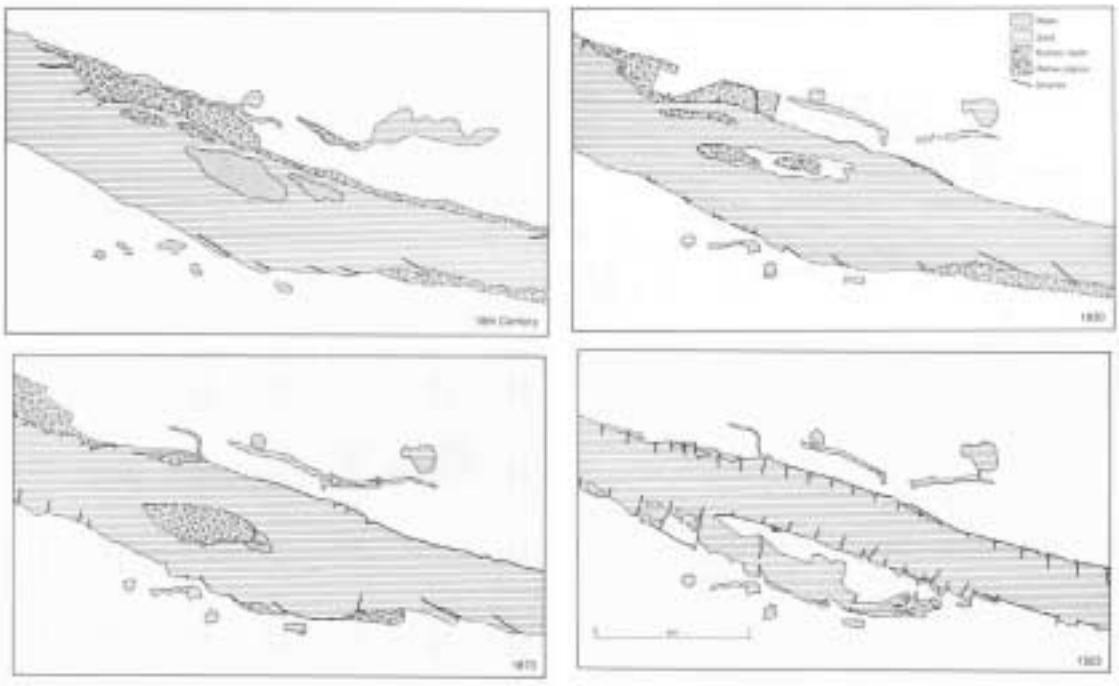

Figure 2-3 The Waal River near Km 892-894 showing the channel changes since the 18th century, source: van Urk & Smit (1989).

What the old maps do not show is the major degradation process going on in the river. The degradation process in the Lower Rhine is complicated; it is mainly due to shortening of river bends, dredging activities, regulation of tributaries, and channel constriction through series of groynes.

Near the entry point of the Lower Rhine to the Netherlands, bed degradation mainly occurred between 1925 and 1960 during that period degradation was about 1.0 m, van Urk & Smit (1989).

The average bed-degradation in the Lower Rhine branches since the end of the normalisation works ranges between 0.4 m to 2.2 m, see Table2-1. Visser (2000) estimated that the bed level of the Rhine branches did not reach equilibrium yet. However, the rate of degradation will be considerably slow when compared to that of the early period after the completion of the normalisation works

Table2-1 Average bed degradation in the different Rhine branches (after, Visser 2000)

River section	Rhine Km	Period	Average degradation (m)
IJssel	878.5 – 1005	1938 - 1990	-0.40
Lek and Neder-Rijn	878.5 – 989	1933 - 1990	-0.90
Pannerden Canal	867.5 – 878.5	1926 - 1990	-2.20
Waal	867.5 – 952	1926 - 1990	-0.70
Boven-Rijn	857.5 – 867.5	1934 - 1990	-1.20

2.3.2. Characteristics of the groyne-fields along the Waal River

Based on field measurements during the years 1996-1997, the Characteristics of the groyne-fields along the Waal River are estimated. With reference to the definition sketch Figure 2-4, the dimensions of the groyne-fields could be defined as (after Schans, 1998):

- A: groyne-field length
- B: groyne-field width
- C: length along the waterline
- D: beach width
- E: distance between the normal line and the thalweg
- F: river width (between groynes)
- G: orientation of a groyne (wrt. the line ⊥ thalweg)
- H: orientation of the groyne-field (wrt. North)

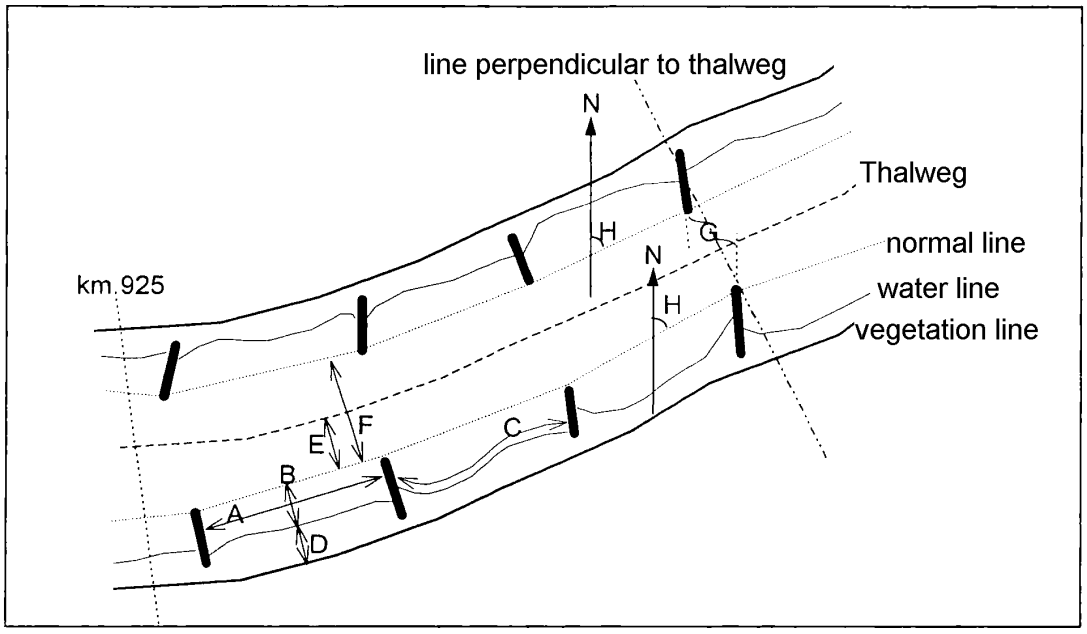

Figure 2-4 Definition sketch for the dimensions of an arbitrary Groyne field, after Schans (1998)

Two more parameters are important for characterising the groyne-fields, viz. the beach slope and the groyne-field bed material size (D_{50}).

Introducing two additional dimensionless parameters, (Schans, 1998), the first is the curvature index (*CI*), and the second will be called the path index (*PI*). The curvature index could be defined as the ratio between the length along the waterline (C) and the groyne-field length (*A*), and it gives an indication about the sinuosity of the beach profile in a groyne-field. *CI* has a minimum of one and the higher it gets the more curved the water line is. The path index (*PI*) could be defined as the ratio between the distance of the thalweg from the groyne (*E*) and the width of the river (*F*). *PI* should always be less be than the unity, and for any value other than 0.50 the thalweg is not in the centreline of the river, (*PI*) gains more importance in curved parts of the river as an indication for the location of the deep part of the river.

$$CI = \frac{C}{A} \text{ and } PI = \frac{E}{F}$$

The characteristics of the groyne-fields along the Waal River could be summarised in Table 2-2, and the accuracy of the measurements of the different parameters is presented in Table 2-3.

Table 2-2 the characteristics of the groyne-fields along the Waal River

Parameter	Mean	Standard deviation	Min.	Max.	Median	Mode
Groyne-field length (A)	198.2	37.7	50	420	200	200
Groyne-field width (B)	67.9	28.6	0	175	65	50
Length along the waterline (C)	215.1	43.5	100	480	210	200
Beach width (D)	25.1	21.2	0	150	20	0
Distance between normal line and thalweg (E)	129.8	93.6	10	320	123.8	25
River width (F)	279.5	35.2	252	412	260	260
Orientation of a groyne (G)	-8.0^o	8.7^o	-30^o	10^o	-5^o	0
Orientation of the groyne-field (H)	86.2^o	31.4^o	2^o	150^o	91^o	96^o
Bed material D_{50} (μm)	439.5	264.5	200	1300	347.5	225
Beach slope	0.042	0.008	0.03	0.05	0.04	0.05
Curvature index (CI)	1.097	0.117	1	1.92	1.056	1
Path index (PI)	0.478	0.338	0.03	0.949	0.046	0.077

Dimensions are in meters

Table 2-3 The accuracy of the different parameters

Parameter	Accuracy	No. of data points
Groyne-field length (A)	± 5 m	799
Groyne-field width (B)	± 5 m	738
Length along the waterline (C)	± 10 m	741
Beach width (D)	± 5 m	734
Distance between normal line and thalweg (E)	± 5 m	736
River width (between groynes) (F)	± 5 m	799
Orientation of a groyne (G)	± 3^o	792
Orientation of the groyne-field (H)	± 3^o	798
Bed material D_{50}	Unknown	46
Beach slope	Unknown	40

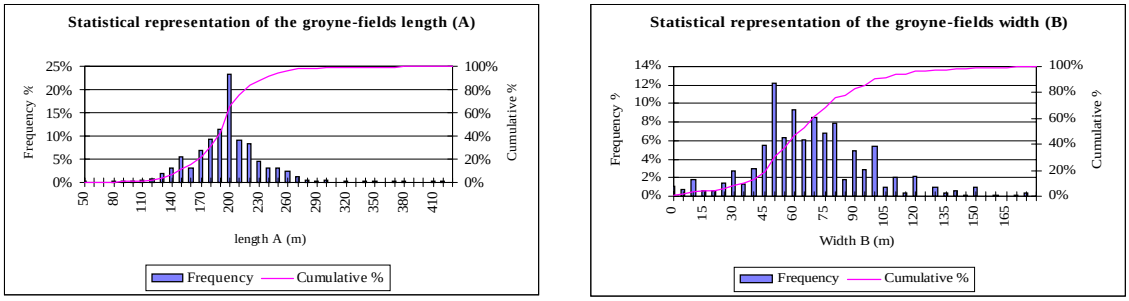

Figure 2-5 Statistical representations for the groyne-fields length (A), and width (B), for the Waal River

Based on the previous analysis and with consideration to the representativeness of groyne-field dimensions, it is possible to assume the following values for a simple geometry that is appropriate to schematise the groyne-fields of the Waal River,

A	≅ 200 m
B	≅ 60 m
D	≅ 25 m
F	≅ 260 m
G	≅ 0^o
H	≅ 90^o
D_{50}	≅ 350 μm
Beach slope	≅ 1:25
CI	≅ 1.0
PI	≅ 0.5

The bed material in the groyne-fields generally consists of well-sorted medium sand with around 70% -by weight- between 250μm and 500μm. At sites which are more exposed to the current, the bed material is less well-sorted and an armour layer of gravel may be found. At these sites, more than 25% of the sediment is coarser than 2.0mm and around 57% is between 125μm and 500μm. The amount of clay and silt in the river bed is insignificant in this stretch of the River Waal the sediments contain no coarse organic material nor any significant amounts of fine detritus.

3. THE EFFECT OF GROYNES ON A RIVER

3.1. FLOW NEAR GROYNES

The flow field near groynes differs significantly in the case of a single groyne from that near a series of groynes.

3.1.1. Flow near a single groyne

The simplest case of groyne layout is a single groyne in a straight reach. The groyne confines a certain part of the river cross section and affects appreciably the kinematic structure of the flow in its vicinity. Mean velocity and specific discharge increase due to the constriction. The increase in the mean velocity leads to a rise in their gradients and more intensive generation of macro-turbulent[*]. Many researchers investigated the flow pattern in the vicinity of a single groyne and found some significant flow characteristics that could be highlighted in the following points:

- Separation region
- Migrating horizontal large eddies
- Water level fluctuation

Geometry of separation region

The characteristics of the separation region formed behind a groyne of non-overflow type were investigated by many researchers, e.g. Ishii et al. (1983), Chen & Ikeda (1997), and Ouillon & Dartus (1997). Such studies gave an impression about the geometry of the separation region downstream a groyne in a rectangular channel.

In a study for the recirculation zone induced by sandbars along the Colorado River, (Schmidt et al. as reported by Chen & Ikeda 1997) subdivided the flow field into four main zones;

- main flow zone
- return flow zone
- shear layer
- reattachment zone

From the tip of the groyne to the opposite channel bank, the flow velocity is accelerated because of the reduction of the channel width. This is called the main flow zone. The return flow zone is located at the downstream side of the groyne, generally with two relatively large eddies. The centre of the larger one is located at a distance of about 6 times the groyne length. The other eddy is smaller, of which the centre is about one time the groyne length. A velocity difference exists between the main flow zone and the return flow zone, which leads to the formation of a shear layer between the two zones.

The reattachment zone is usually simplified by most of the researchers into a point. This point is defined as the point at which the boundary streamline reattaches to the channel boundary. However, the instantaneous reattachment point fluctuates back and forth, mainly due to the intermittence of eddies in the shear layer and the unstable balance of entertainment and pressure gradient between the main flow and recirculation zone. We can regard the point with a maximum instantaneous velocity of zero as the upstream end of the reattachment zone, and the point with a minimum instantaneous velocity of zero as its the downstream end. Chen & Ikeda (1997) observed that the length of the reattachment zone is almost constant and over the range from 11 to 17 times the length

[*] *The description of the macro-turbulence flow structure is related to the local scour problem which is out side the scope of this study*

of the groyne, i.e. the reattachment zone covers a distance of around 6 times the length of the groyne.

Nevertheless, the time-averaged reattachment point could be defined as the point at which the time-averaged velocity is zero. According to Chen & Ikeda (1997) the reattachment point is located at a distance of about 14 times the length of the groyne. In a comparison between numerical model investigation and experimental results, Ouillon & Dartus (1997) reported that -for the experiments- the reattachment length is in the order of 12.5 times the length of the groyne, and it is around 11.5 times the groyne length according to Tingsanchali & Maheswarn (1990).

In an extensive experimental study Ishii et al. (1983), investigated the effect of some dimensionless parameters on the shape of the separation region (only subcritical flow was studied). They reported that the shape of the separation region is hardly affected by Froude number (F_r), and it had dimensions of a length that ranged from 10 to 12 times the groyne length, and the maximum width measured from the sidewall was 2 times the groyne length (for a fixed angle of 90^o, and a relative projected length of 10% from the channel width). Yet, with the increase of the relative projected length to the flow from 10% to 40% of the channel width, the relative separation length decreased from 12 to 7; but the reattachment angle of the boundary streamline by which the main flow and the separation region are bounded remained constant at 15^o.

Furthermore, changing the projection angle of the groyne to the flow from 90^o to 150^o i.e. pointing downstream, the geometry of the separation region remained almost constant. Yet, by decreasing the groyne angle from 90^o to 30^o i.e. pointing upstream, the relative length decreased from 14 to 11, but both the relative width and the reattachment angle remained constant at 2, and 10^o respectively. The upstream separation angle is governed only by the groyne projection angle to the flow. It varies from 30^o to 60^o, for a change of the groyne projection angle from 30^o to 90^o, and remains constant at 60^o for any groyne angle more than 90^o.

From those results, we can deduce that the separation region has a length that could vary from 7 times the groyne length (for relatively long groynes), to 15 times the groyne length. Yet, the relative width is less varying and has a value that is slightly less than two times the groyne length. Depending on the relative wall roughness, the downstream reattachment angle could also vary from 15^o to 10^o with the higher values for relatively high wall roughness. Moreover, the upstream reattachment angle varies from 30^o to 60^o with the variation of the groyne projection angle.

Horizontal large eddies

Another important aspect of the flow field near a groyne is the horizontal large eddies that shed from the tip of a groyne. Through measuring the water level fluctuations along the centreline of the migrating vortices, Chen & Ikeda (1997) found that there is a clear periodic water level fluctuations. These water level fluctuations have a clear phase difference between the signals at two consecutive points along the centreline of the migrating eddies. The lag time between the peak of these two signals is considered the time that a migrating eddy takes to move between those two points. Applying *FFT* method to analyse the periodicity and the time lag between any pair of signals, he found that the average migration velocity of the eddies is nearly constant and takes a value slightly (1.5%) higher than the mean flow velocity.

As the eddies move downstream they merge with each other. Thus, their length-scale increases in the downstream direction. Since the migrating velocity is constant, the time-scale of the eddies should also increase in the downstream direction. Chen & Ikeda (1997) showed the increasing pattern in the time-scale of horizontal eddies, this increase indicates that there is a frequent merging of small-scale eddies after shedding from the groyne tip, until a certain distance and then remaining constant.

Water surface fluctuation

The water surface fluctuates as the horizontal large eddies migrate down stream, that is why the properties of the eddies could be studied by measuring the water surface fluctuation. In general, the

water level increases at the upstream side of the groyne and decreases in the downstream side, and continuously fluctuates as the horizontal eddies periodically shed from the tip of the groyne. Chen & Ikeda (1997) studied the water surface fluctuations though plotting the root mean square of the surface fluctuations at several cross sections downstream of the groyne. For every cross section, he found that there is a peak, which indicates that the centre of the large eddy. However, the influence of the groyne on the water level fluctuations extends to a distance of only 10 times the groyne length.

3.1.2. Flow pattern in groyne-fields

Under conditions where the groynes are not submerged, the groyne-fields are not really part of the wetted cross section of a river. Because of that, the flow pattern in the groyne-field is not directly the result of the discharge in the main channel. Reducing the main stream velocity has no effect on the flow pattern itself, whereas lowering the water level does, Uijttewaal et al. (2001) In the later case the effect of the bottom slope become more pronounced, shifting the eddy centre towards the main stream. Moreover, the flow pattern inside a groyne-field may change with the change of its geometry, location along the river (inner curve, outer curve, or straight part), and/or the groynes orientation, Przedwojski et al. (1995).

However, there is an indirect effect of the discharge on the flow pattern in the groyne-field. Because of the flow that is diverted from the main channel into the groyne-fields, the water flows into the groyne-field with low velocity through the downstream half of the interfacial section between the groyne-field and the main channel. This water flows back to the main channel through a small width of that section, just downstream the upstream groyne of the groyne-field, Termes et al. (1991).

A typical result from one of the experiments done by WL | Delft hydraulics for a groyne-field in a straight section of the river WL|Delft_Hydraulics (1987) is shown in Figure 3-1**.** It shows the flow pattern in a groyne-field with dimensions 200m x 50m, at a river discharge of 1450 m^3/s (representative dimensions and discharge for the Waal River). We can clearly observe a large eddy that covers the first three-quarters of the groyne-field develops directly downstream of the upstream groyne where the main current cannot make a sharp bend into the groyne field. The point around

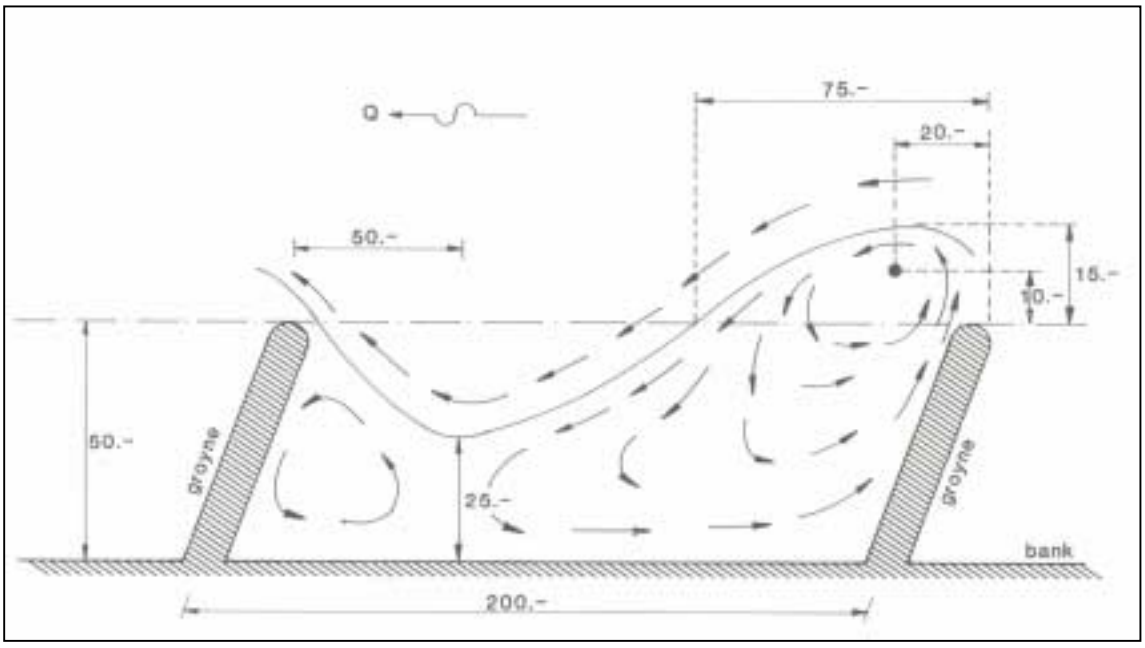

Figure 3-1 Flow pattern in a groyne-field – dimensions in metres, source: Brolsma (1988)

which the eddy circulate, is not really at the centre of the eddy as we may observe, it is very near to the tip of the upstream groyne and dragged towards the main channel. Further downstream, the main current does enter the groyne-field, consequently the stream width becomes larger. A second -smaller- eddy develops at the upstream face of the second groyne where the outflow is hampered by this groyne.

Based on model tests for groynes located along a river bend Klingeman et al. (1984), report that six types of eddy patterns between groynes can be distinguished Figure 3-2**.**

- **Type one:** The circulation pattern of this type is distinguished by the main flow that is deflected outside the groyne field, and a single eddy develops between the groynes. This eddy is well developed and it could prevent the main flow from penetrating the groyne-field. Therefore, this pattern is desirable for navigation purposes as a continuous deep channel is maintained along the face of the groyne field.
- **Type two:** In this type, a second eddy appears but the main current is maintained deflected outside the groyne-field.
- **Type three:** As the spacing between groynes increase, type three-flow pattern develops. The main current is directed into the groyne-field, creating a much stronger eddy near the upstream groyne, and greater turbulence along the upstream face and at the groyne lower head.
- **Type four:** in this type, the stability of the upstream eddy is washed out, and a sing1e strong reverse current occurs.
- **Type five:** In this type the flow, which is diverted by the upstream groyne, is directed to the bank in the groyne-field. Eddies form on both sides of this flow, providing some protection for the bank.

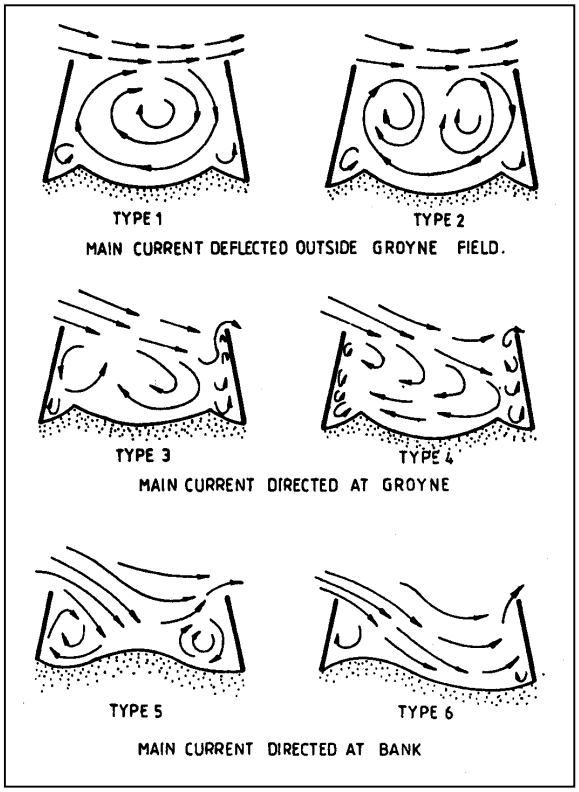

Figure 3-2 Types of flow pattern in groyne-field, source: Przedwojski et al. (1995)

- **Type six**: As the spacing between the groynes further increases, the downstream eddy, which was providing the protection to the bank wanes, and the flow attacks the bank directly.

Furthermore, the maximum velocity along the bank inside the groyne-field of an aspect ratio of 2.5, is roughly 40% of the velocity measured in a similar bend protected by riprap. This percentage is slightly less than 40% when the spacing-length ratio decreased to 1.5, and equal to approximately 50% when the spacing increased to 3.5 times the groyne length.

In his observation on the effect of the geometry on the flow field in a groyne-field, Uijttewaal (1999) concluded that the groyne-field length to width ratio determines the number and shape of eddies that emerge in the stagnant flow region. An aspect ratio close to unity gives rise to a single eddy, (Figure 3-4**,** upper part). A larger aspect ratio gives room for two stationary eddies, a large one called primary eddy, in the downstream part of the groyne-field, and a smaller secondary eddy, emerges near the upstream groyne. The extreme long groyne-field case of length to width ratio of six, shows the penetration of the main flow into the groyne field, (Figure 3-4, lower part). The two eddies remain in a relatively stable position, while the main flow field starts to penetrate into the groyne field further downstream. In all cases, there is an eddy detaches from the upstream groyne

tip that travels along the main channel groyne-field interface and eventually merges with the primary eddy.

The significant difference between the mean, and the instantaneous flow field was highlighted by Uijttewaal (1999). In the upper part of Figure 3-3, the mean flow field obtained a groyne-field with length to width ratio (L/W) = 3. In the downstream part of the groyne-field a large eddy covering two-third of the groyne-field area, is clearly visible. The lower left corner contains a second eddy rotating much slower and in anti-clockwise direction. While in the upper left side where this second eddy borders the main stream, no clear pattern is observed. The indefinite velocity field in this area is mainly due to the averaging process, which obscures the dynamics of the instationary flow. From an instantaneous velocity field as shown in the lower part of Figure 3-3**,** the strong time-dependent motion of a large eddy that is advected through the groyne field is visible. Comparing both figures taken from the same experiment reveals the significant increase in the intensity of the eddy in the case of instantaneous flow field.

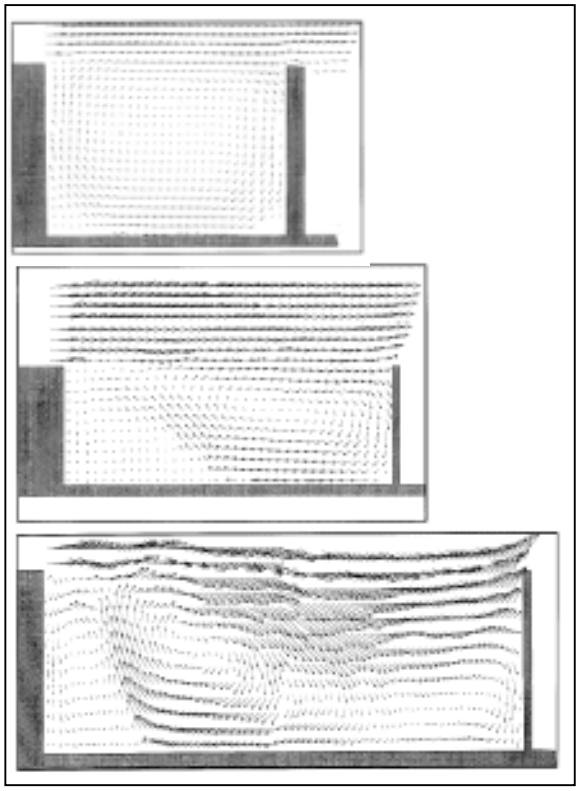

Figure 3-4 Mean flow field in case of length to width ratio =1, 3, 6 consequently, after Uijttewaal (1999)

From the first look, a conflict might appear between the results of the experiments done by WL|Delft Hydraulics (1987) and those of Uijttewaal (1999). However, through a closer look to the original data of WL|Delft Hydraulics (1987), we can conclude that it compares well with the instantaneous flow field reported by Uijttewaal (1999).

Close review to the flow field exhibits the fact that the flow pattern when groynes are not submerged is predominantly two-dimensional. The small-scale three-dimensional turbulence plays a minor role in the mass and momentum exchange process between the groyne-field and the main channel, Uijttewaal (1999). Whereas, no strong three-dimensional large structures are developing obviously due to the shallowness of water, with the exception for the area near the groyne head where the flow is strongly three dimensional, Kerbs et al. (1999).

Moreover, these results emphasise the importance of numerical simulation methods that consider the large-scale dynamics, as the exchange processes is highly affected by the presence of large dynamic structures and their associated mixing length scales. However, the effective length scale associated with the

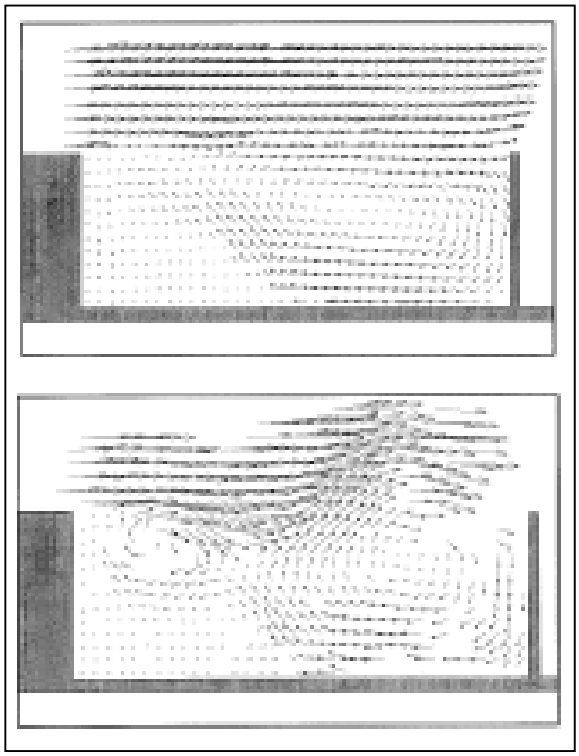

Figure 3-3 Comparison between mean, and instantaneous flow field, after Uijttewaal (1999)

mixing process is hard to determine from Reynolds-averaged simulation models since they do not incorporate the time dependent large-scale motions as shown in the instantaneous flow field. This feature could be dealt with by using, e.g. large eddy simulation.

3.1.3. Submerged groynes

Reviewing the available literature revealed the lack of investigations that deals with groynes during the submerged condition. This might be due to that; the need to investigate the submerged groynes did not arise as the groynes are mostly operating under emerged conditions. Another reason might be the complexity and three-dimensionality of the problem, which require advanced measurement techniques, and/or powerful three-dimensional computational abilities. However, the case of submerged groynes was studied by e.g. Aya et al. (1997), Peng et al. (1997), Krebs et al. (1999), and Tominaga et al. (2001).

Aya et al. (1997), reported a sharp decrease in the water level between the upstream and downstream sides of the groynes, this means that the water surface slope between two successive groynes is less than the slope in the main channel region.

Peng et al. (1997) compared three-dimensional numerical results with experimental results and found that the flow pattern in the case of submerged groynes shows strong three-dimensional features behind groynes. The recirculation size at the back of the groyne is reduced gradually as the top of the groyne is approached. Consequently, the reattachment length decreases from bottom to top plans. The location of recirculation centre also varies in Z-direction. It moves from the tip of the groyne (near the bed), towards the bank (close to the top surface plane). In the upstream face of the groyne, the flow shows an upward motion because of the blockage effect of the groyne.

It should be also noted that the when groynes are submerged the flow over the groynes acts as a damper for the large horizontal structures, ultimately causing it to disappear when reaching a high enough submergence level.

Another important aspect for the flow pattern in the case of submerged groynes, is the secondary flow structure. It occurs simply because of the existences of groynes and the disturbance that it presents. On top of the groyne, the secondary flow (in YZ-plane) has the following characteristics: Near the surface, it is from the bank side towards the mid-channel, and near the groyne top, it is the other way around. Behind the groyne in the recirculation region, the secondary flow also goes towards the mid-channel near the water surface, and near the bed, it is from the mid-channel towards the groyne field as well. Krebs et al. (1999) reported the same feature, they found that in the case of submerged groynes, there is a near bed flow from the mid-channel towards the groyne-field. Yet, in the case of emerged groynes, the secondary flow is negligible.

As mentioned before that the spacing between the groynes affect the flow pattern in the XY-plane; it affects the flow pattern in the YZ-plane as well. Separation flow over the upstream groyne may reattach the groyne-field bed and the bed shear stress recovers its large value (that is usually reduced because of the groynes), if the groynes are spaced far apart. Too close groynes will prevent the flow reattachment to the bed maintaining the bed shear stress at low value, see Peng et al. (1997).

3.2. MORPHOLOGICAL EFFECT OF GROYNES ON A RIVER

3.2.1. General

Erosion can refer to a multitude of natural process, such as soil erosion, beach erosion, or riverbank erosion. It may result from flow of water or air, or from wave action. For localised erosion the word scour is often used, scour at the head of a groyne, at an abutment, or at a bridge pier, etc. A reach of the river may also scour but then it is usually referred to as degradation.

Scour is a localised lowering of riverbed that is usually linked to structures. It could be subdivided to:

- Constriction scour, arising from the constriction of the waterway by the presence of the structure. It changes the cross section geometry in the area near the structure and normally it does not extend to a longer distance.
- Local scour, resulting from the effect of the structure on the local flow pattern and the generation of macro-turbulent in its vicinity. It is always more pronounced than the constriction scour. The local scour maybe – in most cases – superimposed on constriction scour.

Further, the scour may be clear-water scour, or live-bed scour. Clear-water scour refers to conditions when the bed material upstream of the scour area is at rest. Live-bed scour occurs under conditions of general sediment transport i.e. there is a continuous sediment supply to the scour zone.

The term degradation, in contrast to scour, implies a lowering of the riverbed that extends over a long distance. Degradation may progress in the downstream direction, upstream direction, or in both directions. For example, the construction of a dam would cause downstream propagating degradation, lowering the downstream water level would cause degradation that propagates in the upstream direction. Usually, channel bed degradation is accompanied by change in the river slope.

When a series of groynes is constructed, the bed forms near the groynes change because of the combined effect of bed degradation due to the long constriction, and the local scour at the end of each groyne. Bed degradation due to long constriction of an alluvial channel as well as, the local scour phenomena near a single groyne has been discussed by many researches. Yet, the overall bed degradation caused by a series of groynes, which have characteristics of both long constriction and a single groyne was discussed by very limited number of researchers. In the following section, we will present the morphological impact of groynes on a river.

3.2.2. Bed Degradation Caused By Long Constriction

Channel bed degradation that is originated from the construction of series of groynes is normally dealt with as a long constriction scour. The effect of reducing the channel width is to increase the bed shear stress, which would result in a considerable scour within the constricted reach. If the constriction is long and permanent, the scour develops to an extended reach of the river (degradation) and its effect further extends to affect the entire river.

Several analytical models have been proposed to compute the constriction scour, One of the earliest works that presented a simplified one-dimensional model theory of the equilibrium depth for a long constriction is due to Straub (1934). Several analytical investigations were conducted on this problem e.g. Komura (1966), Gill (1981), Bhowmik (1989), and Klaassen (1995).

Komura (1966) and Gill (1981) exclusively extended the approach of Laursen and reached nearly similar expression for the constriction scour. Komura (1966), investigated the effect of different sediment sizes (D) and the standard deviation of the particle size distribution (σ_ϕ), his expression reads:

$$\frac{d_2}{d_1} = \begin{cases} \left(\frac{B_1}{B_2}\right)^{(6/7)} \left(\frac{\tau_1}{\tau_2}\right)^{(3/7)} \left(\frac{D_1}{D_2}\right)^{(-1/7)} & \text{clear-water} \\ \left(\frac{B_1}{B_2}\right)^{(6/7)} \left(\frac{\tau_1}{\tau_2}\right)^{(2/7)} & \text{live-bed} \end{cases}$$

LANE'S BALANCE

Another way to evaluate the ultimate response of the river to a long constriction, or any other change in the forcing parameters, is the use of the so-called "Lane's balance". It was first introduced by Lane in 1955, see Jansen et al. (1979), Bhowmik (1989), and Klaassen (1995). The basic theory behind it is that for any stable stream, a balance exists between the water discharge (Q), gradient (i), sediment load (S), and the bed load material size (D). This relation takes the form, [$\boldsymbol{S.D::Q.i}$] where "**::**" means "is proportional to". This relation could also be derived analytically through the application of the four equations describing the time and space dependant behaviour of a river. The four equations are the conservation of water mass, conservation of water momentum, conservation of sediment mass, and the equation of sediment motion, Jansen et al. (1979). Later, the original Lane's balance was modified by Klaassen (1995), who derived it analytically to include more parameters. The expressions are then read:

i. For the slope (i):
$$S \cdot D^p \cdot B^{\frac{n-3}{3}} = m \cdot C^{\frac{2n}{3}} \cdot Q^{\frac{n}{3}} \cdot i^{\frac{n}{3}}$$

ii. For the water depth (h):
$$S \cdot D^p \cdot B^{n-1} = m \cdot Q^n \cdot h^{-n}$$

Where, the exponents (n) and (p) depend on the sediment transport predictor. The value of (n) ranges from 2 to 5 for high values of bed shear stress; n = 5 for the England & Hansen (1967) formula. For the same formula, (p = 1), and for the formula of Meyer-Peter & Muller (1948) (p) takes the following form:

$$p = \frac{3}{2} \frac{0.047}{\theta' - 0.047}$$

iii. To include the effect of yearly discharge variation:
$$V \cdot D^p \cdot B^{\frac{n-3}{3}} = m \cdot C^{\frac{2n}{3}} \cdot i^{\frac{n}{3}} \cdot N \sum_{i=1}^{n} P_i \cdot Q_i^{\frac{n}{3}}$$

Where:

$$V = \int_{1 year} S.dt$$

N is the number of seconds in a year
P_i is the probability of occurrence of the discharge Q_i

Applying this concept for the simple case of a constant water discharge and sediment discharge leads to the following expressions for the slope and depth variations of the constricted reach:

$$\frac{d_2}{d_1} = \left(\frac{B_2}{B_1}\right)^{-\frac{n-1}{n}}$$

$$\frac{i_2}{i_1} = \left(\frac{B_2}{B_1} \right)^{\frac{n-3}{n}}$$

3.2.3. Bed Degradation Caused By Series of Groynes

The channel bed degradation caused by a series of groynes could be treated as a long constriction scour. However, due to the formation of separation flow zone around the tip of every groyne the effect of groynes as a constriction to the channel is slightly different from that of a solid long constriction. Michiue et al. as reported by Suzuki et al. (1987), introduced a multiplication factor (λ) that modifies the constriction width caused by the construction of a series of groynes into its equivalent constriction width by a solid constriction. The multiplication factor (λ) takes the following values:

$$\text{for} \frac{S}{L} \to 0 \qquad \lambda \to 1$$

$$\text{for} \frac{S}{L} \to \infty \qquad \lambda \to (\frac{B_0}{B_1})$$

Where (*S*) is the spacing between groynes, (*L*) is the groyne length (B_0) is channel width, and (B_1) is the constriction width ($B_1 = B_0 - L$).

Based on flume experiments for series of groynes, Suzuki et al. (1987) showed that when the ratio (*S/L*) is very small the groynes work as a group. On the other hand, when (*S/L*) is very large each groyne works independently. When (*S/L*) is between 4 and 8, the channel bed degradation is almost the same by that of a long constriction i.e. (λ = 1). When (*S/L*) is less than 4, bed degradation is larger than that of a long constriction i.e. (λ < 1), while it becomes smaller when (*S/L*) is greater than 8 i.e. (λ > 1).

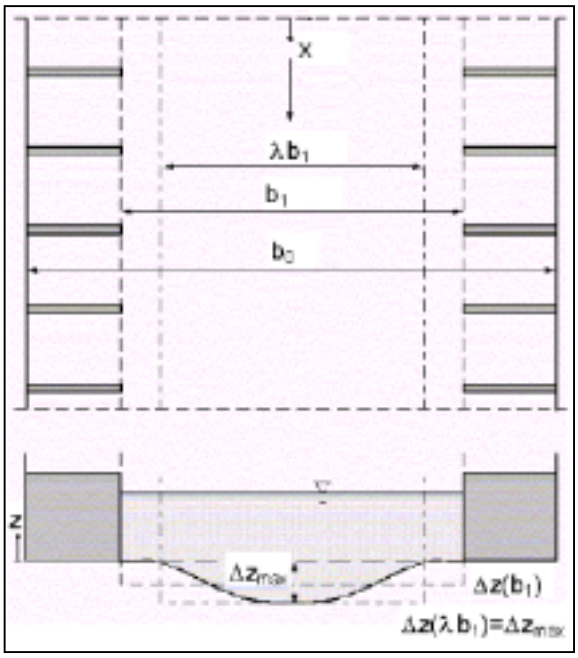

Figure 3-5 Definition of the coefficient (λ), source: Spannring (1999)

Wang & Yanapirut (1988), carried out similar experiment to study the effect of the ratio (*S/L*), he covered the range from (*S/L*) = 1.67 to (*S/L*) = 5.0. He analytically derived the static equilibrium bed degradation formula (reached before by other authors) of $\left\{ \frac{d_2}{d_1} = (\frac{B_1}{B_2})^{6/7} \right\}$. Moreover, he extended his formulation through dimensional analysis and dimensionless plots to include the ratio (*S/L*), his formula reads:

$$\frac{d_2}{d_1} = \left(\frac{B_1}{B_2} \right)^{6/7} \cdot \left(\frac{S}{L} \right)^{-1/7}$$

Spannring (1999), applied Komura's formula of equilibrium degradation depth to calculate the coefficient (λ) introduced earlier by Suzuki. From known values for Δz_{max} resulting from numerical computations, the corresponding values for (λ) could be determined. The resulting groyne coefficients are in a narrow range with a mean value of λ = 0.78 and a their standard deviation is σ_λ = 0.02. Further, he commented that the cross section profile could be approximated by a 4th degree parabola.

3.2.4. Local Scour Near Groynes

One of the characteristic features of groynes is the local scour that occurs in they vicinity. The process of local scour around abutments, and groynes could be divided into several phases: initial phase, development phase, stabilisation phase, and equilibrium phase, Hoffmans & Verheij (1997). Two important characteristics are the equilibrium depth and the time evolution of scour.

Equilibrium scour depth

In order to estimate the maximum depth of scour, many formulae have been developed. Extensive review and detailed comparisons between the different formulations of local scour around abutments and spur- dikes is given by; among others Gill (1972), Darghi (1982), Noshi (1997), Klingeman et al. (1984), and Hoffmans & Verheij (1997).

Through laboratory experiments, several researchers independently reached at similar expression for the equilibrium scour depth near groynes. The expression takes the form, $d(\infty) = K \cdot q^{2/3}$ see for example Gill (1972), Klingeman et al. (1984)and Hoffmans & Verheij (1997). For example, the expression of Ahmed as given by Hoffmans & Verheij (1997) reads:

$$y_{s,e} + h_0 = K_A \cdot K_A^{`} \cdot \left(\frac{q}{1-m} \right)^{2/3}$$

Where:

$y_{s,e}$ = equilibrium scour depth below initial depth
h_0 = initial water depth
m = b/B, b and B are the width of the dike and channel respectively.
$K`_A$ = $2.14g^{-1/3}$ ($\cong 1.0\ m^{-1/3}.\ s^{2/3}$)
K_A = $2K_p\ K_s\ K_\alpha\ K_\mu$
K_p = correction factor for the influence of channel bend, (inner = 0.85, outer = 1.1~1.4)
K_s = for the shape of structure, (vertical wall = 1.0, 1:1 sloped =0.85)
K_α = for the angle of attack, (30^o to 150^o = 0.80 ~ 1.10)
K_μ = for the influence of porosity (0.2 porosity =1.0, 0.5 porosity =0.9~0.6)

The previous expression for local scour estimation was based on experimental work, and dimensional analysis techniques. It lacked the theoretical background and missed some parameters that proved to be of importance. Laursen**,** who contributed many researches about local scour problem, emphasised the importance of the distinction between clear-water conditions, and live-bed conditions in the estimation of scour depth. A factor that was considered in the above mentioned treatments.

Gill (1972), through analytical approach extended the formulation of Straub. He distinguished between clear water condition, where the bed shear stress is less than then the critical bed shear stress ($\tau_1 < \tau_c$), and live bed condition where ($\tau_1 > \tau_c$). Moreover, Gill introduced the effect of the sediment size (D), and the sediment transport capacity formula exponent (n) (of $s = m.u^n$). His form reads:

$$y_{s,e} + h_0 = h_0 \cdot \begin{cases} \alpha \left(\frac{1}{1-m} \right)^{(6/7)} \left(\frac{\tau_1}{\tau_c} \right)^{(3/7)} & \text{clear-water} \\ \alpha \left(\frac{1}{1-m} \right)^{(6/7)-(3/7n)} & \text{live-bed, } \tau_c >> \tau_1 \end{cases}$$

From the laboratory measurements, he found that,

$$\alpha = 8.375\left(\frac{D_{50}}{h_0}\right)^{0.25}$$

Hoffmans & Verheij (1997) compared a large number of scour predictors with experimental data and proposed the following formula:

$$y_{s,e} = h_0\left(\left(\frac{1}{1-m}\right)^{\frac{2}{3}} - 1\right) + K_B \cdot b \cdot \tanh\left(\frac{h_0}{b}\right)$$

With ($y_{s,e}$) as the scour below the original depth and (K_B) correction factor ≅1.5 for groynes with sloped face, and $m = b/B$, b and B are the width of the dike and channel respectively.

Local scour depth for a series of groynes

When a bank is protected with a series of groynes, the scour depth varies with the groyne location. The local scour depth near a groyne that is far downstream from the first groyne is different from that of a single groyne. However, the scour depth around the first groyne is similar to that of a single groyne. Because of the influence of the neighbouring groynes, the scour depth usually becomes smaller than that of the single groyne. Suzuki et al. (1987), showed through laboratory experiments, that the local scour depth around a groyne located far downstream in a series of groynes is a function of the groyne spacing (S) to length (L) ratio, and it could be expressed roughly in the following form:

$$\frac{Z_{s,DS}}{Z_{s,1}} = 0.07 \cdot \frac{S}{L} + 0.14 \qquad \text{for } 2 < \frac{S}{L} < 10$$

Where:

$Z_{s,\,DS}$ = scour depth around any groyne far downstream.
$Z_{s,\,1}$ = scour depth around the first groyne which is similar to the scour depth near a single groyne and could be estimated using any of the above mentioned formulae.

When (S/L)>12, i.e. the groynes are very far apart, the group action vanishes and the scour depth near any groyne is nearly the same as that of a single groyne.

Przedwojski (1995) investigated the bed topography and the local scour at groynes in two bends of the Warta River. He found that the local scour depth varies with groyne location, and the maximum depth occurs at the groyne located downstream of the bend apex. The longitudinal variation of scour depth at groynes located along the outer bank of a bend is quite similar to the bed level changes due to the bend curvature. The scour depth changes depend significantly on the flow and bed topography in a given bend. Moreover, based on the analysis of the field investigations he estimated that the variation on the scour depth along a bend takes the following relation:

$$y_{s,e} = \beta \cdot H\left[\frac{h_0}{H} + \frac{Q_g}{Q_0}\cos(2\pi \cdot \frac{x}{L}) + \sin(\alpha - 90)\right]^{n-2}$$

Where:

- β = coefficient (β = 0.275 as given by Przedwojski (1995))
- α = angle between groyne axis and flow direction
- n = exponent of sediment transport formula ($s = m.u^n$)
- H = average reach flow depth
- h_0 = unperturbed flow depth
- L = bend length
- x = distance from the bend entrance
- Q_0 = discharge over the bottom width between groynes

- Q_g = part of the discharge blocked by the groyne $\left(Q_g = h_0 U S \sin\frac{\Delta\varphi}{2}\right)$
- S = spacing between two groynes
- U = unperturbed velocity at the toe of the groyne
- $\Delta\phi$ = angle between two successive groynes

Extended review for local scour problem is given by Przedwojski et al. (1995) and Hoffmans & Verheij (1997).

Time Scale for Scour Development

For abutment with a length that is more than the water depth (same as groynes), Hoffmans & Verheij (1997) proposed the following formula, which is valid for all scour phases:

$$\frac{y_s}{y_{s,e}} = 1 - e^{a\left(\frac{t}{t_s}\right)^{\gamma}}$$

In which:

$y_{s,e}$ = equilibrium scour depth below initial depth [m]
y_s = maximum scour depth at any time (t) [m]
t_1 = characteristic time at which $y_m = h_0$ [s]
γ = constant ≅ 0.40

and, $a = \ln\left(1 - \frac{h_0}{h_0 + y_{s,e}}\right)$

From dimensional analysis and the results of many experiments, he found that:

$$t_s = \frac{K \cdot h_0^2 \cdot \Delta^{1.7}}{(\alpha U_0 - U_c)^{4.3}}$$

In which:

K = coefficient (K = 330 *hours* $m^{2.3}.s^{-4.3}$, then t_1 is expressed in hours)
Δ = relative density
α = coefficient depends on turbulence intensity
U_0, U_c= mean, and critical velocities [m/s]

The α-factor is given in Hoffmans & Verheij (1997) to range from 2 to 9 according to the geometry of the groyne.

Scour Geometry

As the geometry of scour near groynes is not of much importance to the research, reference is made to some researchers who treated this point.

Rajaratnam (1983), through experimental work described the bed shear stress distribution in the vicinity of a groyne, he noted an increase in the shear stress value up to 5.2 times the values in the undisturbed locations.

Kuhnle et al. (1999) studied the effect of normal/overtopping flow conditions in the laboratory. He deduced detailed topographic maps showing the geometry of the scour/deposition near groynes, and predicted the area and volume of scour holes. He further commented that the larger the overtopping ratios caused the region of maximum scour to shift towards the channel bank and caused a secondary scour zone to form downstream of the groyne.

Peng et al. (1999) studied the scour and deposition around submerged groynes through numerical simulation and compared his results with experimental results. He noted that the scour develops rapidly at the initial stage, 78% of the equilibrium depth was reached within 25% of the equilibrium

time. Moreover, he presented the transverse and longitudinal profiles of the scour hole, and noted that the eroded sand deposited just downstream the scour hole.

Klingeman et al. (1984) tested different orientations and found that the shape and area of scour is strongly related to the orientation of the groyne to the flow.

4. HYDRAULIC DISTURBANCES CAUSED BY NAVIGATION

In a river like the River Rhine, which is considered the backbone of NW European waterways network, navigation is very important element affecting the morphology of both the groyne-fields and the main channel. It is ought to be included when attempting to investigate the interaction between the groyne-fields and the main channel.

4.1. NAVIGATION INDUCED WATER MOTION

Before discussing the navigation induced water motion near groynes, some attention will be given to the water motion around a ship and the associated water level variations.

4.1.1. Water movement around a ship

As a vessel navigates through a waterway, it generates hydraulic disturbances in the form of waves and currents. The dominant hydraulic disturbance features associated with a moving tow are the drawdown, return current, propeller jets, and secondary waves. The drawdown and the return current together form the ***primary water movement.*** The ship-induced waves form the ***secondary water movement.*** The size of the vessel with respect to the waterway along with its speed dictates the magnitude of these forces and their effects on the environment, Bhowmik et al. (1995), Hochstein & Adams (1989).

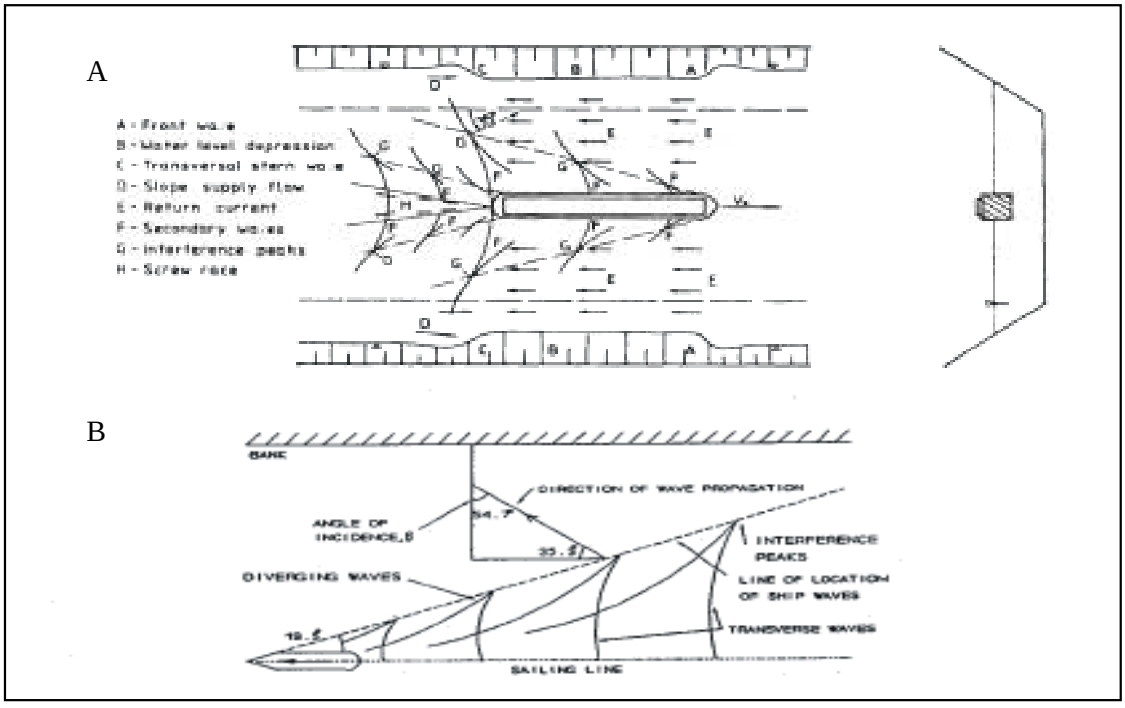

Figure 4-1 Ship-induced water motion in a restricted waterway, source:Przedwojski et al. (1995)

As the vessel displaces water during its forward motion, it causes a drop in the water level alongside the barges known as the drawdown, Figure 4-1A. Drawdown begins near the bow and rebounds near the stern producing a single wave with a duration on the order of 40 to 120 sec, depending on vessel length. Drawdown can cause dewatering of shallow areas along the shoreline during vessel passage.

The maximum return current is produced adjacent to the barges and typically closer to the stern. As vessels move upstream, return currents cause a temporary increase in ambient current velocities.

In a tow moving downstream, the return current causes a decrease in ambient current velocities and under certain low flow conditions can create temporary ambient flow reversals. Currents associated with the propeller jets are highly three-dimensional and cause localised disturbances to the flow. The characteristics of these jets are a function of the hull shape, propeller type and size, and horsepower of the vessel. The thrust, alignment to the bank, and the rudder angles affect the potential flow impingement on the bed or banks. Under normal underway operations, propeller jet effects are limited to the area behind the tow in the navigation lane.

Beginning at the corners of the lead barges, waves diverge from the sides of the tow. As transverse stern waves intersect with this diverging wave, secondary waves are formed which propagate away from the tow at an angle toward the shoreline, Figure 4-1B. These waves are rather consistent in amplitude and have short periods (1 to 5 sec.). For high-speed vessels, these waves can have significant wave heights and often dominate the hydraulic disturbances produced by the vessel. Transverse waves diminish in magnitude with distance from the stern and have wave periods on the order of 2 to 5 seconds. The influence of waves will diminish as the return current and water-level depression are enlarged. In this way, the smaller and faster ships are usually responsible for bank erosion due to the secondary waves, while the larger and slower ships cause erosion due to the return current.

4.1.2. Return current and water level depression

A ship moving along a restricted waterway with a relative velocity (V_s) will induce a return current (E) and a water level depression (B), see Figure 4-1. In accordance with Bernoulli theorem, the higher the return current velocity, the lower the water level will get in the vicinity of the vessel. Using the continuity principle and the Bernoulli equation, the average values of the return current velocity (U_r) and the water level depression (Δh), can be expressed in Schijf's form, more details are given by Przedwojski et al. (1995) and Groeneveld (1997).

$$U_r = V_s\left(\frac{A_c}{A_w} - 1\right)$$

$$\Delta h = \frac{V_s^2}{2g}\left[\alpha\left(\frac{A_c}{A_w}\right)^2 - 1\right]$$

Where:

$$\alpha = 1.4 - 0.4\left(\frac{V_s}{V_{\lim}}\right)$$

A_c = undisturbed waterway cross sectional area
A_w = waterway cross sectional area during a ship passage = ($A_c - \Delta h.B - A_m$)
A_m = cross sectional area of water replaced by the vessel
B = undisturbed waterline width
V_s = vessel speed
$V_{\lim}$ = vessel limit speed = $\left[(0.5 \sim 0.75)\cdot\sqrt{gh}\right]$

These equations can be solved by iterative procedures, or by the use of design curves, see Groeneveld (1997). The maximum values of return current velocity ($U_{r,max}$) and the water level depression (Δh_{max}), are dependant on the ship type. For the pushtow units, Verheij & van der Wal (1984) found that:

$$U_{r,\max} = C \cdot U_r$$

$$\Delta h_{\max} = C \cdot \Delta h$$

Where:

$$C = 1.2 + 5 \cdot 10^{-4} \cdot Fr_h \cdot \frac{B}{y_t} \cdot \frac{L_s^2}{h\sqrt{A_m}}$$

Fr_h : Froude number related to water depth = $\frac{V_s}{\sqrt{gh}}$

y_t : distance between vessel axis and waterway bank
L_s : Length of the vessel

A review for the different formulations to compute the return flow due to navigation traffic is given by Bhowmik et al. (1995) and Hochstein & Adams (1989). For the Waal River conditions the model given by Hochstein & Adams (1989) seems to be most applicable, ten Brinke et al. (1999). Later Ten Brinke used it to compare between the measured and computed current velocities in the groyne-fields along the Waal River. Yet, he found that the **actual** measured maximum current velocities are much **higher** than the computed near bank current velocities (even higher than the computed average return flow in the river). Further, he concluded that it could not be applied to navigation traffic in the Waal River. However, the model of Hochstein & Adams (1989) reads:

$$U_r = V_s \cdot \left(\left[(a-1)B + 1 \right]^{0.5} - 1 \right)$$

Where:

$$a = \left(\frac{n}{n-1} \right)^{2.5} \quad \text{with,} \quad n = \frac{A_c}{A_m}$$

$$B = \begin{cases} 0.3 \cdot e^{1.8\frac{V_s}{V_{cr}}} & \text{for } \frac{V_s}{V_{cr}} \le 0.65 \\ 1 & \text{for } 0.65 < \frac{V_s}{V_{cr}} \le 1.0 \end{cases}$$

for the Waal River B =1.0

V_{cr} is the so-called vessel critical velocity and takes the following form:

$$V_{cr} = K \left(\frac{g \cdot A_c}{B_c} \right)^{0.5}$$

B_c = channel top width
K = constrainment factor = f(*n*, vessel dimensions), for the Waal River $K \cong 0.70$

The shape of the lateral flow velocity distribution could be represented by the following relation:

$$U_r(y) = k_1 \cdot e^{-\frac{y}{k_2}}$$

Where:

$$k_1 = U_r(0) = \alpha \cdot U_r$$

$$k_2 = \frac{y_s}{\alpha(1 - e^{-\alpha \cdot f(\alpha)})}$$

$$\alpha = \max \begin{cases} 0.114\frac{B_c}{b} + 0.715 \\ 1.0 \end{cases}$$

$$f(\alpha) = 0.42 + 0.5 \ln \alpha$$

$U_r(y)$ = return flow velocity at a distance (y) from the centreline of the vessel
y_s = distance between the vessel centreline and the bank

b = vessel width

4.1.3. Ship waves

Secondary waves are induced by ships moving with a relatively high speed, they comprise diverging and transverse waves. The result of interference of these waves is known as interference peaks or ship waves. The direction of propagation of the peaks makes an angle of 35 degrees to the bank line. (Verheij & Bogaerts, 1988) as reported by Przedwojski et al. (1995), showed that the interference peaks are very similar to wind waves, despite their origin. The wave height of those peaks at the bank could be taken as:

$$H_i = \alpha_i \cdot h \cdot \left(\frac{h}{y_s} \right)^{0.33} \cdot Fr_h^4 \quad For\ V_s < 0.8V_{lim}$$

Where:

y_s = distance between the side of the vessel and the bank
α_i = coefficient depends on the shape of the vessel
α_i = 1.0 for tugs, patrol boats, and loaded conventional inland motor vessels)
α_i = 0.5 for empty European barges
α_i = 0.35 for empty conventional motor vessels

The above expression is based on Kelvin's theory for deep-water conditions. The same theory used for calculation of the wave length gives:

$$L_w = 0.67 \cdot \frac{2\pi}{g} \cdot V_s^2 \qquad \text{(Valid only for } Fr_h < 0.7, \text{ and } H_i < 0.67h)$$

And the wave period,

$$T = \sqrt{\frac{2\pi L_w}{g}}$$

An expression that relates the maximum bottom wave orbital velocity to wave height, length, and period is given by (van Rijn, 1993):

$$\hat{U} = \frac{\pi \cdot H_i}{T \cdot \sinh(kh)}$$

$$k \text{ (wave number)} = \frac{2\pi}{L_w}$$

h = the water depth

4.2. EFFECT OF NAVIGATION ON THE FLOW IN A GROYNE-FIELD

In the previous section, the basic components of navigation induced water motion was introduced for an ideal case of a ship sailing near the centreline of a rectangular channel section. Yet, in a natural river, the situation is rather complex, a number of factors; for side slope effect, eccentric sailing course, and natural irregularities has to be introduced to convert the simplified case into the more complex one. Further, if groynes exist, the estimation of navigation-induced water motion is even more complex.

Some attempts were made to understand the navigation induced water motion, and its effect on the sediment motion from the beaches of the groyne fields prior to the introduction of the six-barge pushtow units to the River Waal. Field measurements during a trial year were carried out see,

Havinga et al. (1984), in addition to laboratory experiments WL|Delft_Hydraulics (1987) to investigate the effects that those units would cause. Dimensions for the different pushtow formations are given in Table 4-1. A computation methodology for the navigation-induced water motion in a groyne-field, including the wave propagation through the groyne-field, is described in details by Termes et al. (1991).

Table 4-1 dimensions for different pushtow formations

Formation	***2x2***	***3x2***	***2x3***
Length (m)	193.0	229.5	193
Breadth (m)	22.8	22.8	34.2
Draught (m)	2.7	2.7	2.7

Figure 4-2**,** shows three important stages during the passage of a pushtow sailing upstream. The return current is a maximum immediately after the bow passes a groyne. The return current is furnished by water from the upstream groyne field and the groyne field alongside. An eddy develops at the groyne head and the small vortex at the downstream end of the groyne field apparently disappears entirely. As the push-boat passes by the supply flow refills the groyne-field. When the stern of the push-boat passes the particular groyne-field, the supply flow is forced to flow out of the groyne field by the upstream groyne, perpendicular to the axis of the fairway. The natural eddy immediately downstream of the groyne is transported downstream by the main current.

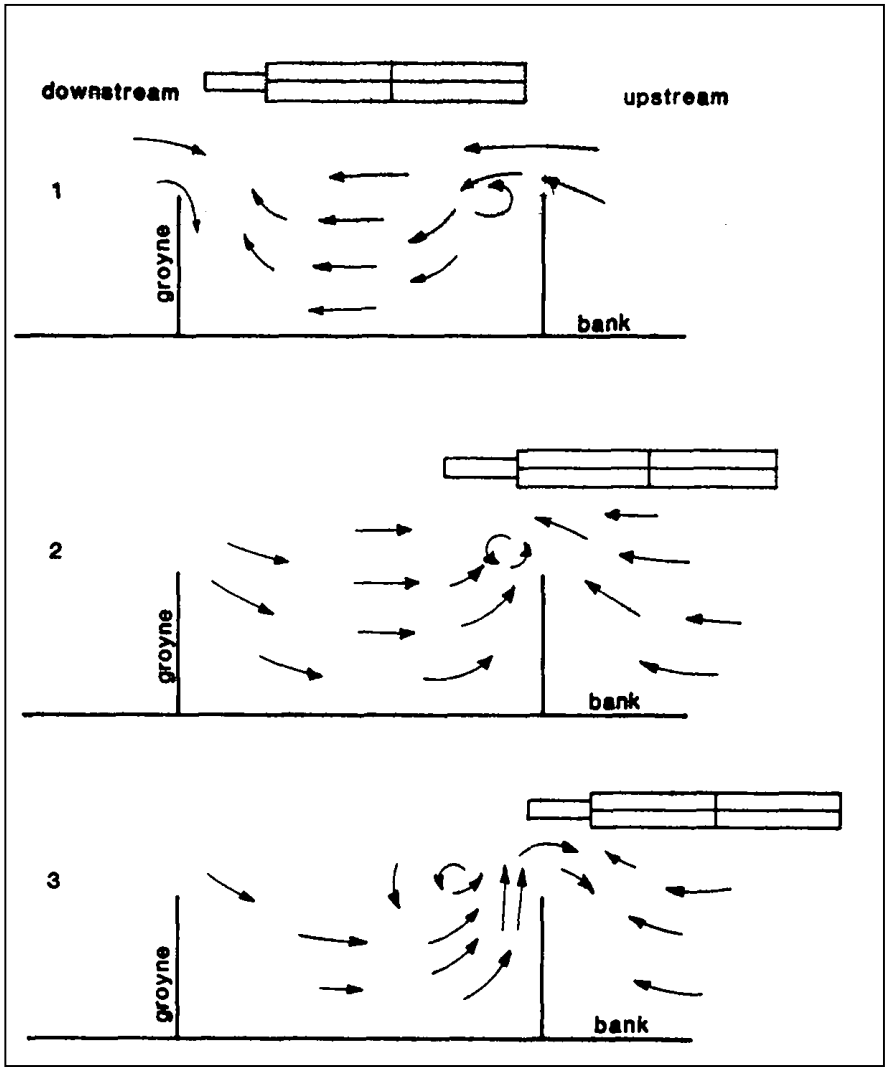

Figure 4-2 Flow pattern in a groyne-field during passage of a pushtow unit, source: Brolsma (1988)

The magnitude of the velocities in the complex ship-induced water movement depends on, ship dimensions, draught, unit speed, distance between pushtow and groyne, dimensions of the groyne field and the river discharge.

In a physical model study performed by WL|Delft_Hydraulics (1987) , see also Brolsma (1988), the navigation-induced water motion for three different formations, namely (3x2), (2x2), and (1x2) were investigated, Figure 4-3. In addition, field measurements during the trial year 1984, to study the effect of (2x2), (3x2), and (2x3) formations on the flow in groyne-fields were carried out by Havinga et al. (1984). From both, the following remarks could be emphasised:

- The increase in return and supply flows can be expected to cause larger velocities mainly just downstream of the groynes. Therefore, increase in ship speed, dimensions and draught will increase the flow velocity near groynes.

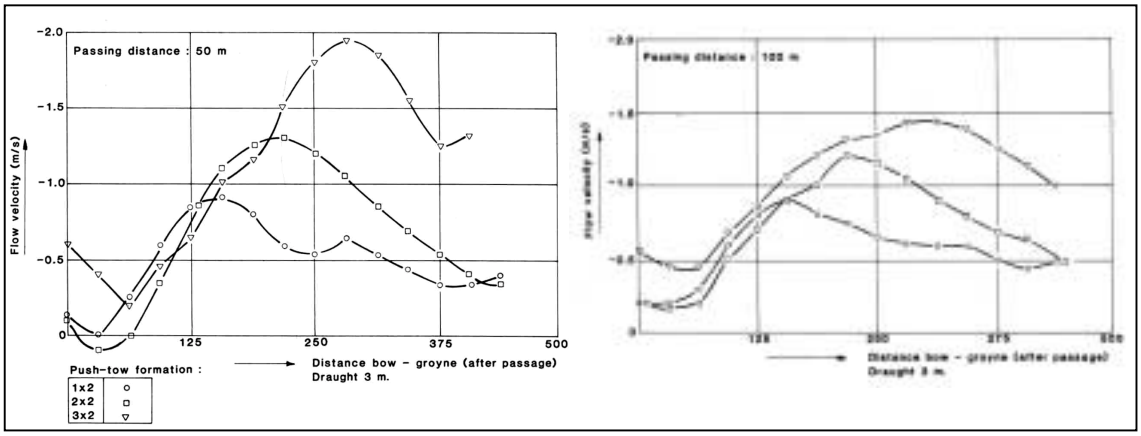

Figure 4-3 Flow velocities during a pushtow passage, source: Brolsma (1988)

- The flow velocities in both (X), and (Y) directions, increase almost linearly with the increase of the relative navigation speed for all the tested formations.
- The model results demonstrated the effect of the passing distance, where the velocities increase with decreasing distance between the ship and the groyne.
- The experiments showed that the maximum current velocities in small groyne-fields are less than in large groyne-fields, because of the smaller effect of the supply flow.
- From the field measurements, the current velocity in the groyne-field was recorded during the passage of all three types. The (2x2) formation produced a maximum return current of 1.10 m/s, 2 to 3 times higher than that with no navigation. The wide formation (2x3) had a lesser effect than the long one (3x2), however they both produced higher current velocity than the (2x2) formation. The long formation yielded an increase in the current magnitude of 45% than the (2x2) formation i.e. 1.6 m/s, and the wide formation increased the current only by 15% i.e. 1.25m/s.
- The water surface decline was also reported by Havinga et al. to be almost the same for the three above-mentioned formations. Around 27cm near the tip of the groyne, and around 20cm near the bank.
- The field experiments further indicated that whereas pushtows tended to produce a considerable increase in the flow in the groyne field, the largest self-propelled ship (about 2000 tons) had very little effect.
- When the river discharge increases, the river cross section also increases. This increase causes a relative reduction of the return current and supply flow caused by navigation. Thus, a reduction of the navigation induced flow velocities occurs. In addition, the relative draught (blockage) decreases, which is also a factor in favour of reducing the navigation effect.

From the field measurements by ten Brinke et al. (1999), the effect of a push-two combination passing a groyne-field was also observed. It induced a water level depression of 15~20 cm, in addition to a drawdown current of 30~40 cm/s (*less than what was reported by Havinga et al. there is no clear reason for that*). This current was strong enough to resuspend the sediment of the groyne-fields beach. An example of the effect of navigation on current velocities, water level fluctuations, and suspended sediment concentration is shown in Figure 4-4. The effect of a pushtow unit passage on the sediment concentration, water level depression, and the return current velocity could be observed during the time 11:5 to 11:20. These results are in analogy with the results obtained from the field measurements of Havinga et al. (1984).

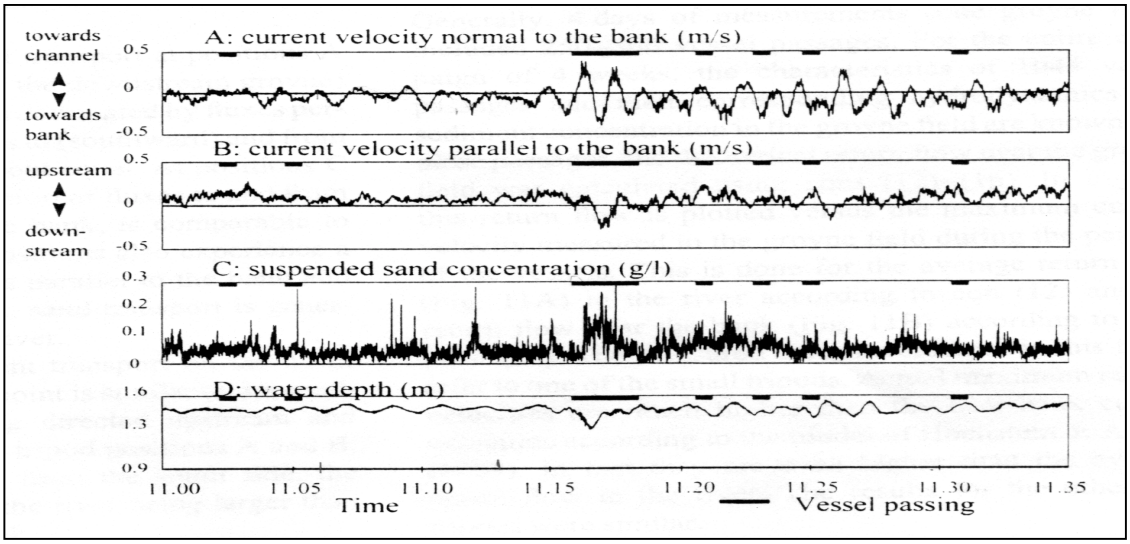

Figure 4-4 Example of the field records showing the navigation effect on current velocities, water level, and sediment concentration, source: ten Brinke et al. (1999).

5. MORPHOLOGICAL INTERACTION BETWEEN THE GROYNE-FIELDS AND THE MAIN CHANNEL

5.1. GENERAL

The morphological interaction between the groyne-fields and the main channel, is a typical Dutch problem. In most rivers, this interaction is insignificant and not perceived as a problem. After the construction of the groynes, the river experiences large-scale deepening. Meanwhile, sand deposits between the groynes form a stable beach. However, in the Waal River the shipping density is among the highest of all the inland waterways of the world. Ships passing through the Waal some times have a length that is more than the distance between two groynes, and they often sail relatively close to the groynes. This results in pronounced sediment transport from the groyne fields to the main channel.

The morphological interaction between the groyne-fields and the main channel is a combination between the effect of navigation and the effect of river flow. At different discharges, the relative effect of the various forcing parameters is different. Erosion of sand is thought to take place due to currents and waves induced by navigation traffic. Deposition of sediment probably takes place mainly at times of high discharge, when the groynes are completely submerged. During these events, sediment is transported from the main channel to the groyne-fields and further landward to the floodplain, (ten Brinke et al. 1999). As long as erosion and deposition are in equilibrium on a time-scale of a couple of years, the beaches between the groynes are in dynamic equilibrium. This has been the case over the last several decades in the Dutch part of the Rhine River. However, this situation may change if the balance between the hydrodynamic forces changes. This could happen if, for example, the navigation intensity changes or the discharge distribution between the branches of Rhine changes, 'which is unlikely to happen'. Changing the geometry of the existing groynes by lowering, shortening, extending, etc. is also a change that could affect the morphodynamics of the river.

Studies to understand the interaction between the groyne-fields and the main channel are scarce in the literature. Moreover, the focus is on understanding the effect of navigation on the morphology of the groyne-fields only during low water conditions. This is one side of the process, which causes erosion of groyne-fields beaches, as the effect of navigation dominates. On the other hand, t the author's knowledge there are no studies 'up to my current knowledge', that discuss the process during high water conditions. Thus, the question of how much sediment is restored to the beaches of the groyne-fields during a flood could not be answered yet.

The effect of navigation on the morphology of the groyne-field was investigated through field measurements, (Havinga et al., 1984), (de Haas & van Essen, 1987a; 1987b), and (ten Brinke et al., 1999) and through model tests (WL|Delft_Hydraulics 1987). A conclusion that they all agreed on, is the complexity and difficulty of describing this phenomenon. In addition, there is a large uncertainty in the estimated sediment transport during a ship passage.

5.2. ESTIMATION OF EROSION FROM GROYNE-FIELDS

In the following two sections, we will present the results of some field campaigns, as well as some attempts to analytically describe the interaction between the main channel and the groyne-fields. On the first section, we will give a summery of the results that were reached through field measurement campaigns. In the second section, we will present some analytical expressions describing the interaction between the groyne-fields and the main channel. Field data analysis is a very important tool to study a phenomenon, and to have an overview of system behaviour under the conditions that are prevailing during the measurements. Thought in many cases interpolating these results could be done successfully, extrapolating them could yield significant errors. Often

a better understanding to the physics behind the phenomena is reached through analytical models. In general, analytical models are rather simplified; yet, they give a comprehensive grasp of the physics behind the phenomena. Combined with field data and physical model results they yield a powerful tool of analysis and prediction.

5.2.1. Field studies

One of the earliest investigations for the morphological changes in groyne-fields is due to Bruin (1977) – after Havinga et al. (1984). Who mentioned that the groyne-fields erosion for the reach Hulhuizen-Zaltbommel of the River Waal is about $3 \sim 4*10^6$ m^3 during the period 1960 through 1976 (i.e. 17 years). This estimate was based on photos at low water conditions. This sediment volume is equivalent to an average lateral supply of sediment to the main channel of about $7.5*10^{-3}$ m^3/s.

During the field measurements carried out by Havinga et al. (1984), it was noticed that only pushtow units cause an increase in the flow velocity that could bring the sediment inside the groyne-fields into motion. To have an idea about the sediment transport volume from a single groyne-field due to a ship passage, we will use the information about Hulhuizen-Zaltbommel reach given in Table 5-1. Utilising that erosion is fully due to pushtow units, we can then deduce that a single groyne-field loses about 0.14 m^3 of sand per passage. In that specific reach, the net changes in the river bed level between the normal lines during the period 1960 through 1976 is known to be negligibly small. During that period, the bottom level in the reach Hulhuizen–Nijmegen (15 Km) dropped by around 0.20 m, and in the reach Nijmegen–Zaltbommel (57 Km) a bottom rise of ca. 0.06 m occurred. Therefore, the erosion value estimated by Bruin (1977) appears to be overestimated.

Table 5-1 information about Hulhuizen-Zaltbommel reach

Distance Hulhuizen-Zaltbommel	65 Km
Number of groyne-fields	560
Frequency of pushtow units	8/day
Groyne-fields erosion (1960-76)	4.10^6 m^3/17 years

Havinga et al. (1984) measured the sediment concentration and the flow velocity during a ship passage; the study area is shown in Figure 5-1. They were aiming to quantify the effect of increasing the capacity by introducing six-barge pushtow units to the navigation fleet. Based on these measurements, they found that for pushtow units, the sediment transport duration is about 60 seconds, and the sediment outflow is primarily through the upstream part of the groyne-field. They estimated this length to be around 20 m, in addition to some outflow from the downstream part directly after the passage of the unit. Further, they estimated the sediment flux from groyne-fields to the main channel per passage for the different pushtow formations. Summery of the results from Havinga et al. (1984) is presented in Table 5-2. These values would lead to an estimate of the erosion volume from the groyne-fields nearly 40%, of that estimated by Bruin (1977).

Table 5-2 Sediment transport from a single groyne-field due to navigation (the effect of different formations)

Formation	***Max. transport 10^{-6} m^2/s***	***Sediment out flux m^3/passage***
2x2	*9.8*	*0.035*
3x2	*19.6*	*0.070*
2x3	*12.0*	*0.040*

Additional conclusion from Havinga et al. (1984) is the effect of the formation geometry on the amount of sediment transport during its passage. With reference to section 4.2, a long formation causes much stronger return current that lasts for a longer period than a shorter formation. Consequently, its associated sediment flux from a groyne-field is much larger than that of the shorter one.

Moreover, they reported that the bottom material is generally at rest in the absence of navigation where the velocity does not exceed 0.2~0.3 m/s as a threshold value. In addition, groyne-fields are supplied with sediment in a much less quantity from the main channel during the periods when there is no ship passages. This supply takes place across the downstream part, primarily due to the primary eddy.

De Haas & van Essen (1987a) studied the groyne-fields in a straight reach of the Waal River near Druten, Figure 5-1. His results conformed to the same conclusion that, there is a sediment supply from the river in the absence of navigation. In this case, the measurements were carried out during a relatively high discharge condition (2000 to 3000 m^3/s). Consequently, the estimated recharge of sediment was relatively high, i.e. in the order of $3.6*10^{-5}$ m^3/s for each groyne. Still the effect of navigation was higher, but no quantitative results could be obtained.

In addition to the study of a straight reach near Druten, de Haas & van Essen (1987b) studied the groyne-fields in a curved reach near St. Andries, where the groynes are located at the outer bend, Figure 5-2. In this case, no sediment recharge from the river, on the other hand, erosion was observed. This is clear as the groynes are located already in the deep part of the cross section and the helical flow structure in a bend is in favour of eroding the groyne-fields that are located at the outer bend.

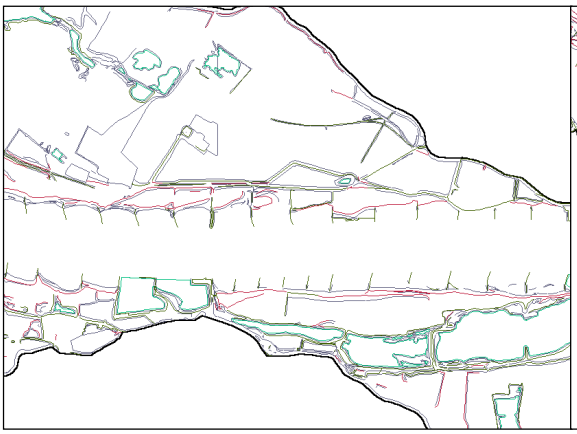

Figure 5-1 River Waal near Druten

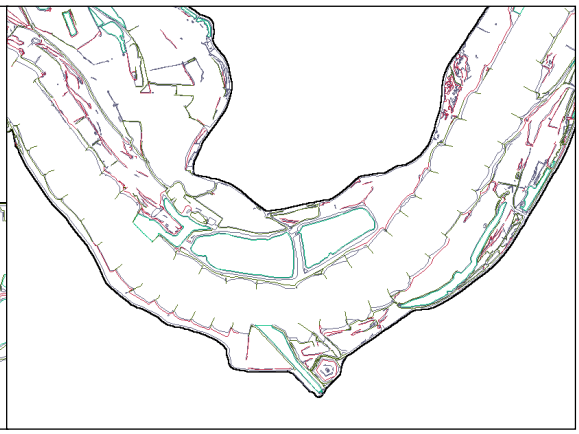

Figure 5-2 River Waal near St. Andries

The most recent field investigation is due to Ten Brinke (1999). He carried out field measurements in the area shown in Figure 5-1. A sample result of his measurements is shown in Figure 4-4, in which it is clear that the turbidity peaks coincides with the passage of a pushtow unit. He estimated an average sand transport from a single groyne-field to be 4.5 kg/s ($0.003 m^3/s$), for 15% of the time. This value is equivalent to 0.18 m^3/passage (with passage time of 60 seconds), compared to the values in Table 5-2, i.e. 2.5 times higher than the maximum value estimated Havinga et al. (1984).

Further, they used this value to estimate a sediment budget from the groyne-fields to the main channel. For roughly 500 sandy groyne-fields along the banks of the Waal, this would result in a total input volume of $7*10^6$ m^3/year. Compared with a yearly sand transport of $0.5*10^6$ m^3/year, this is clearly far too much. The reason for this exaggerated estimation could be one or more of the following reasons:

- The study was carried out during a relatively low discharge, around 1000 m^3/s compared with 1467 m^3/s as a mean value. This means that the effect of navigation is relatively high, as the effect of navigation increases with the decrease of the water level.

- The study area is in a straight reach of the river and cannot be generalised for the entire river. As the groyne-fields behaves differently according to their location along the river. A groyne-field in a bend behaves significantly different from that in a straight reach. The location in the bend, i.e. inner curve or outer curve has a great effect.
- For the estimation of the total sediment volume, the total year was used as a base time, and the effect of the discharge stage was not considered. During relatively high discharges, the effect of navigation could be neglected. This would lead to decreasing the time at which there is erosion of the groyne-fields.

5.2.2. Analytical approach

The first analytical representation to the problem is due to Havinga et al. (1984), primarily to investigate the impact of using six-barge pushtow units. It is based on a comparative approach between the impact of the navigation induced water motion for the four-barge units, and that of the six-barge units. They considered that the current situation is a result of the effect of the four-barge units. Comparing, the maximum return current velocity because of the two formations, and taking the existing bed level inside the groyne-fields as a reference level. They estimated that the use of six-barge units would lead to bed lowering for the groyne-fields beaches in the order of one to two meters. No comment will be given on this model as it is based on very crude assumption.

Based on the concept of mass conservation, WL|Delft_Hydraulics (1987) proposed an analytical model to the problem. The model is divided into two different parts. The first part describes the sedimentation of groyne-fields by normal flow. The second part treats the problem of groyne-field erosion. Both parts are dealing with the non-submerged conditions.

Sedimentation of groyne-fields

In the first part of the model, the navigation effect is not present and the bed is assumed to be aggrading due to an inflow sediment flux. The sediment flux is assumed to take place through the downstream part of the groyne-field. Integrating the sediment concentration (*s/q*) over the inflow length and depth, the total inflow sediment volume could be estimated. Due to the eddies that are dominating the flow inside the groyne-field, sediment is assumed to be distributed uniformly throughout the whole groyne-field area (L_{gf} x B_{gf}), the temporal bed variations (Z_{gf}/ *t)* could then be estimated. The assumptions behind the model are based on the results of a physical model investigation. With reference to Figure 5-3, they are as follows:

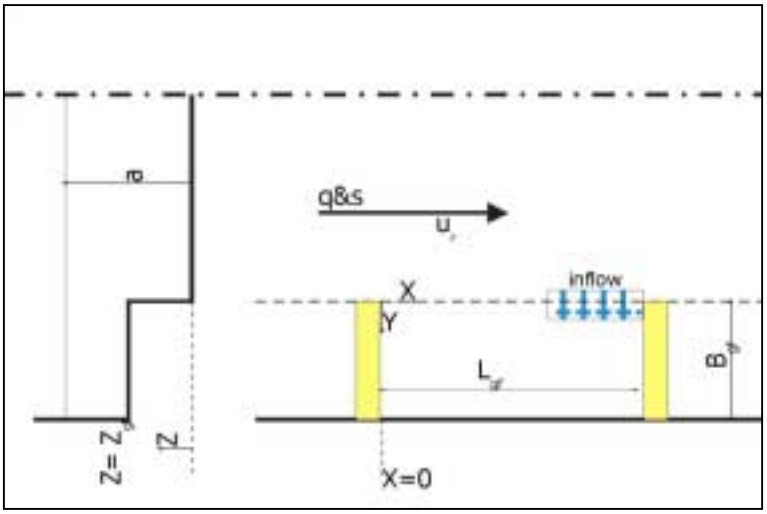

Figure 5-3 Definition sketch for the model of WL|Delft Hydraulics (1987)

- Active inflow length is only 20% of the total groyne-field length, the last 20% of the groyne-field length (L_{gf}).

- The inflow velocity (u) is 35% of the stream velocity (u_r), i.e. $u = 0.35 * u_r$.

Integrating the inflow velocity and the sediment concentration (c) over the length and depth of the groyne-field;

$$B_{gf} \cdot L_{gf} \cdot \frac{\partial Z_{gf}}{\partial t} = \frac{1}{(1-\varepsilon)\cdot \rho_s} \cdot \int_0^{L_{gf}} \int_0^{a} u(x,z)\cdot c(x,z)\cdot dz \cdot dx$$

with inflow concentration (c_i);

$$c_i = \rho_s \cdot (1-\varepsilon) \cdot \frac{a - z_{gf}}{a} \cdot \left(\frac{s}{q}\right)$$

and, inflow discharge;

$$\Delta Q = \underbrace{0.2 \cdot L_{gf}}_{\text{active length}} \cdot \underbrace{0.35 \cdot u_r}_{\text{inflow velocity}} \cdot \underbrace{(a - z_{gf})}_{\text{water height}} \cdot$$

introducing the constant (A_1);

$$A_1 = \frac{0.07 \cdot u_r}{B_{gf} \cdot a} \cdot \left(\frac{s}{q}\right)$$

reducing the double integration to;

$$B_{gf} \cdot L_{gf} \cdot \frac{\partial Z_{gf}}{\partial t} = \frac{1}{(1-\varepsilon)\cdot \rho_s} \cdot \Delta Q \cdot c_i$$

Consequently, the groyne-fields bed level temporal variations read:

$$\frac{\partial Z_{gf}}{\partial t} = A_1 \cdot (a - Z_{gf})^2$$

This equation has the following solution, with a graphical representation in Figure 5-4.

$$Z_{gf} = a - \frac{1}{A_1 \cdot t + \left(\frac{1}{a - z_0}\right)}$$

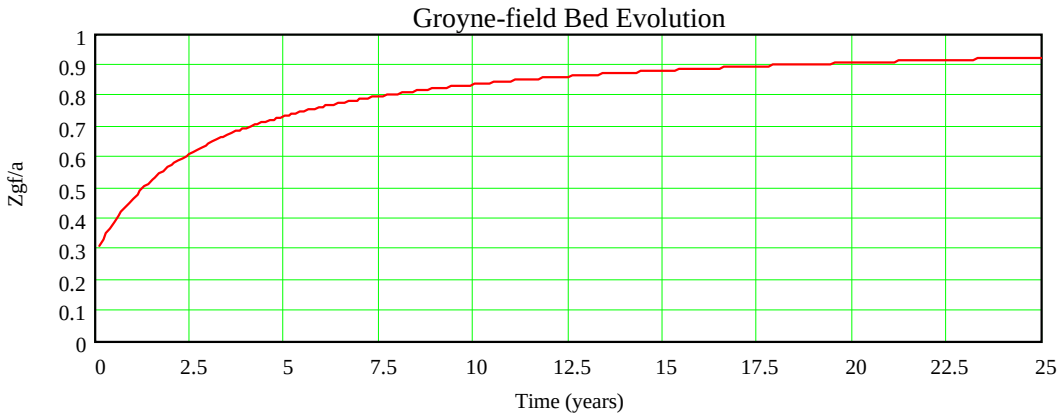

Figure 5-4 Groyne-field bed aggradation in the absence of navigation

Note that for time (t), the solution of this equation is ($Z_{gf} = a$) i.e. the groyne-fields will be completely filled with sediment. This is not true, but it is a direct result for the assumptions underlying this model.

Erosion of groyne-fields because of Navigation

The second part of the model of WL|Delft_Hydraulics (1987), treats the problem of groyne-field erosion. In which the effect of navigation as a forcing parameter that creates an additional outflow velocity which transports sediment out from the groyne-field. The outflow velocity (v_*), is maximum (v_{max}) near the tip of upstream groyne (sailing wise), and reduces exponentially with the distance towards the downstream groyne.

In the same manner like the first part, integrating the sediment transported throughout the whole groyne-field length, and over the passage time of a vessel. Utilising England&Hanesen sediment transport predictor formula, the total erosion volume (E) from a groyne-field during a ship passage time (T) could be written in the following form;

$$E = \int_0^{T_s} \int_0^{L_{gf}} m v_*^n \cdot e^{\delta \cdot (x - L_{gf})} \cdot dx \cdot dt$$

by integration;

$$E = \frac{T_s \cdot m v_*^n}{\delta} (1 - e^{-\delta \cdot L_{gf}})$$

Assuming that the term $(e^{-\delta \cdot L_{gf}})$ is negligible, the temporal bed variation due navigation induced erosion will take the following form:

$$\frac{dZ_{gf}}{dt} = -\frac{f_s \cdot T_s}{B_{gf} \cdot L_{gf} \cdot \delta} \cdot (m \cdot v_{\max}^n)$$

Where:

f_s : frequency of navigation;
T_s : vessel passage time;
δ : reduction parameter;

and by integration;

$$Z_{gf} = z_0 - \frac{f_s \cdot T_s}{B_{gf} \cdot L_{gf} \cdot \delta} \cdot (m \cdot v_*^n) \cdot t$$

This is a linear relation with time, and it gives rise to unacceptable results for large values of time. This is a result to the absence of any slowdown mechanism. For example, if the outflow velocity is a function of the groyne-field bed level, and the sediment transport formula has a threshold value, eventually the bed degradation will converge to an equilibrium value. In the last step, i.e. the integration of the *DE*, all parameters were considered constant with time. However, if the effect of the discharge stage on the navigation-related parameters is implicitly introduced, a better definition might be reached.

Equilibrium bed level

For reach a definition for the equilibrium bed level we will equate the erosion rate with the deposition rate.

$$\left(\frac{\partial z_{gf}}{\partial t} \right)_{\text{erosion}} + \left(\frac{\partial z_{gf}}{\partial t} \right)_{\text{deposition}} = 0$$

simplifying and introducing a constant (A_2);

$$A_2 = \frac{m \cdot a^2}{0.07 \cdot L_{gf} \cdot s \cdot \delta}$$

We reach a definition for the equilibrium bed level (Z_{eq}) that reads:

$$Z_{eq} = a - \sqrt{A_2 \cdot f_s \cdot T_s \cdot V_*^n}$$

Furthermore, by combining the two definitions reached for the temporal variations of both erosion and deposition, we reach at a definition that describes the long-term variations of the groyne-fields bed level, see Figure 5-5. The definition reads:

$$\frac{\sqrt{A_3}}{A_1} \cdot \ln\left[\frac{1+\sqrt{A_3}(a-Z_{gf})}{1-\sqrt{A_3}(a-Z_{gf})}\right] = t + \frac{\sqrt{A_3}}{A_1} \cdot \ln\left[\frac{1+\sqrt{A_3}(a-z_0)}{1-\sqrt{A_3}(a-z_0)}\right] \quad \text{for } \left|\sqrt{A3} \cdot (a-Z_{gf})\right| < 1$$

$$\frac{\sqrt{A_3}}{A_1} \cdot \ln\left[\frac{1+\sqrt{A_3}(a-Z_{gf})}{\sqrt{A_3}(a-Z_{gf})-1}\right] = t + \frac{\sqrt{A_3}}{A_1} \cdot \ln\left[\frac{1+\sqrt{A_3}(a-z_0)}{\sqrt{A_3}(a-z_0)-1}\right] \quad \text{for } \left|\sqrt{A3} \cdot (a-Z_{gf})\right| > 1$$

With the constant (A_3);

$$A_3 = \frac{A_1 \cdot B_{gf} \cdot L_{gf} \cdot \delta}{f_s \cdot T_s \cdot (m \cdot v_{\max}^n)}$$

Figure 5-5 Long-term variation in groyne-fields bed level

This representation of the combined effect of flow and navigation induced sediment motion inherits the deficiencies of both parts. The groyne-field bed level converges to the equilibrium bed level (z_{eq}) which is directly defined by equating both of them.

Finally, the model of (WL|Delft_Hydraulics 1987) has some deficiencies as we mentioned before and it might lead to unrealistic results. In addition, it is very sensitive to some parameters such as the reduction parameter (δ), navigation frequency (f_s). However, the basic idea and the assumptions behind it are valuable and it forms a base for further development to remove the deficiencies.

The model of Sieben & Douben

Another model is proposed by Sieben & Douben (2000). A complete derivation is given in Appendix II. They estimated the equilibrium groyne-field bed level to take the form,

$$\frac{\Delta z}{a} = A + B \cdot \ln\theta$$

where, A and B are constants, and θ is the Shields parameter.

Furthermore, they attempted to estimate the effect of the interaction between the groyne-fields and the main channel on the morphology of the main channel he arrived at the following expressions:

$$\left[1-\frac{c\,k}{(1-\varepsilon)}\frac{L_g}{B_{mc}}k\,(1-\frac{\Delta z}{a})^2\right]\cdot\frac{\partial z_{mc}}{\partial t}+\frac{u}{a}\frac{dq_s}{du}\cdot\frac{\partial z_{mc}}{\partial x}=\left[\frac{L_g}{B_{mc}}\frac{1}{(1-\varepsilon)}\left(c-c\,k(1-\frac{\Delta z}{a})-1+\varepsilon\right)\right]\cdot\frac{\partial z_{gf}}{\partial t}$$

$$\left[1-\frac{c\,k}{(1-\varepsilon)}\frac{L_g}{B_{mc}}k\,(1-\frac{\Delta z}{a})^2\right]\cdot\frac{\partial z_{mc}}{\partial t}+\frac{u}{3i}\frac{dq_s}{du}\cdot\frac{\partial^2 z_{mc}}{\partial x^2}=\left[\frac{L_g}{B_{mc}}\frac{1}{(1-\varepsilon)}\left(c-c\,k(1-\frac{\Delta z}{a})-1+\varepsilon\right)\right]\cdot\frac{\partial z_{gf}}{\partial t}$$

The first for the small-scale (*simple wave model*), and the second for the large-scale effect (*parabolic model*). Moreover, he estimated the morphological time-scale for the groyne-field bed variations to take the following definition:

$$T_m=\frac{a}{k\cdot w`}\cdot\frac{(1-\varepsilon)}{\chi\cdot(\frac{q_s}{q})}$$

where, T_m [s] is the morphological time-scale. Sieben & Douben (2000) estimated that for the groyne-fields bed variations under the Waal River conditions is about 50 days.

5.3. EFFECT OF CHANGING THE EXISTING GROYNES GEOMETRY

The possible effects of lowering the groynes, lengthening or shortening, and decreasing their spacing were investigated by Verheij (1997). He concluded that groyne lowering has the greatest influence at water levels between the old and the new crest heights. It would also lead to some aggradation in the main channel. In an outer bend, the groyne lowering could result in a small reduction of the width of the fairway and in some depth reduction for part of the channel section. Compared to the present situation, lowering of the groynes has a negative effect on the siltation after a high water.

5.3.1. Lowering the groynes

The effect of a lowered groyne height is negligible as long as the water level remains below the lowered groyne height (average 50 to 70% of the time depending on the level of the crest). As soon as the water level is higher than the lowered level the groynes will be over flooded and a part of the total discharge will pass over the groynes through the groyne fields. This has both positive and negative impacts.

As positive effect, the flow capacity will be better and there will be a milder velocity gradient through the mixing zone between the main channel and the groyne-fields. It is as well, expected that the contribution of the discharge passing over the groynes and through the groyne field, will increase the conveyance capacity of the river. Further, the local scour holes forming near the tip of the groynes will be less deep due to the reduced specific discharge and the reduced maximum water depth at which the groyne is not yet submerged. Consequently, the sedimentation downstream of the scour hole forming the so called “groyne flames” will be reduced.

As a negative effect, the discharge in the main channel will drop compared to the initial situation (1D-effect), and the effective stream width will be larger. This results in a tendency to general aggradation in the main channel, as the flow velocity will be lower. In an outer bend, during times that the water level is higher than lowered groyne level, more water will flow through the groyne fields and for a longer period, compared with the not-lowered groynes. This might lead to an increased sediment flux towards the floodplain.

Additionally, as the morphological interaction between the groyne-fields and the main channel due to navigation is not fully understood, the impact of lowering the groynes 'from this point of view' cannot be predicted. In the light of the above section (5.2), the groyne-fields bed generally erodes due to navigation during low water conditions, and during high water conditions deposition occurs. The transition of the behaviour from bed erosion to deposition and vice versa, is strongly related to the groynes crest level. Lowering the crest level would affect the existing balance between the two forcing parameters. The result is not really known.

5.3.2. Lengthening or shortening of groynes

Extending the groyne length results in general sense in larger water depths in the main channel compared to the original groyne length. Lengthening can limit the width of the fairway depending on the local situation. Shortening leads to opposite effects compared to lengthening. Lengthening a series of groynes over a long reach is 'to some extent' similar to long constriction, i.e. the river bottom will drop over that reach. This has a negative morphological impact on the upstream part; further, the water surface slope will change. However, lengthening or shortening of one or few groynes is a local operation and has limited impacts in both upstream and downstream of it.

Changing the dimensions of groynes will indeed change the geometry of the groyne-fields. Consequently, the large turbulent structures that are governed by groyne-fields length to width ratio will also change. However, with a small change in the groyne length (in the order of 10 to 20m) this effect is negligible. In general, groynes lengthening or shortening have positive and negative consequences. Yet, for navigation purposes groyne shortening appears to be not desirable, groyne lengthening may be considered favourable.

5.3.3. Decreasing the groynes spacing

With reference to section 3.1.2, the large horizontal eddy structure is determined by the aspect ratio of the groyne-field's dimensions. Reducing the groynes spacing will permit a single 'more stable' eddy that is confining the streamlines to a relatively smaller width. The morphological impact on the main channel is minor, yet it would cause some degradation. Another effect that is not clear at the moment, is the effect on the navigation induced water motion and its accompanying sediment transport. In the one hand, we would expect a more protection to the groyne-fields of less spaced groynes. On the other hand, there might be a stronger water level depression, and more confined outflow, that would then transport more sediment out of the groyne-fields.

The distance between the groynes should be specified mainly by the required stability of the separation flow line with various discharges. A considerable reducing of the groyne spacing leads to an increase of the water depth in the main channel by a few percent. The length of the scouring hole will specify the minimum spacing between the groynes.

REFERENCES

Alvarez, J. A. M. (1989). "Design of groins and spur dikes." *Proceedings 1989 National Conference On Hydraulic Engineering*, New Orleans, 296-301.

Aya, S., Fujita, I., and Miyawaki, N. (1997). "2-d models for flows in river with submerged groins." *27th IAHR Congress*, San Francisco, CA. USA, 829-837.

Bhowmik, N. G. (1989). "Phsical impacts of human alterations within river basins - the case of the kanakakee, mississippi and illinois rivers." *XXII IAHR Congress*, Ottawa, Canada, B139-B146.

Bhowmik, N. G., Xia, R., Mazumder, S., and Soong, T. W. (1995). "Return flow in rivers due to navigation traffic." *Journal of Hydraulic Engineering, ASCE*, 121(12), pp. 914-918.

ten Brinke, W. B. M., Kruyt, N. M., Kroon, A., and van den Berg, J. H. (1999). "Erosion of sediments between groynes in the river waal as a result of navigation traffic." *Spec. Publs int. Ass. Sediment*, 28, pp. 147-160.

Brolsma, J. U. (1988). *Six-barge pushtow trials*, PIANC, Den Haag.

Chen, F. Y., and Ikeda, S. (1997). "Horizontal separation in shallow open channels with spur dikes." *Journal of Hydroscience and Hydraulic Engineering*, 15(2), pp. 15-30.

Darghi, B. (1982). "Local scour around bridge piers - a review of theory & practice." *TRITA-VBI-114*, Royal institute of technology, Stockholm, Sweden.

Gill, M. A. (1972). "Erosion of sand beds around spur dikes." *Journal of Hydraulic Engineering, ASCE*, 98(HY9), pp. 1587-1602.

Gill, M. A. (1981). "Bed erosion in rectangular long contraction." *Journal of Hydraulic Division, ASCE*, 107(HY3), pp. 273-284.

Groeneveld, R. (1997). "Inland waterways - ports, waterways and inland navigation." *CT4330*, Delft University of Technology, Delft.

de Haas, A. D., and van Essen, J. A. F. (1987a). "Onderzoek naar de invloed van duwvaart op de water- en zandbeweging in het kribvak durten." *DBW/RIZA 87.007*, RIZA, Arnhem.

de Haas, A. D., and van Essen, J. A. F. (1987b). "Onderzoek naar de invloed van duwvaart op de water- en zandbeweging in het kribvak st. Andries." *DBW/RIZA 87.008*, RIZA, Arnhem.

Havinga, H., Slootweg, H., and Zeekant, J. (1984). "Kribvakmeting t.B.V. Zesbaksduwvaart op de waal bij druten." *84.9*, Rijkswaterstaat, district Zuidoost, Arnhem.

Hochstein, A. B., and Adams, E., Jr. (1989). "Influence of vessel movements on stability of restricted channels." *Journal of Waterway, Port, Coastal, and Ocean Engineering, ASCE*, 115(4), pp. 444-456.

Hoffmans, G. J. C. M., and Verheij, H. J. (1997). *Scour manual*, A.A. Balkema, Rotterdam.

Ishii, C., Asada, H., and Kishi, T. (1983). "Shape of separation region formed behind a groyne of non-overflow type in rivers." *XX IAHR Congress*, Moscow, USSR, 405-412.

Jansen, P. P., van Bendegom, J., van den Berg, J. H., de Vries, M., and Zanen, A. (1979). *Principles of river engineering - the non tidal alluvial rivers*, Delftse Uitgevers Maatschappij, Delft.

Klaassen, G. J. (1995). "Lane's balance revisited." *6th International Symposium on River Sedimentation*, New Delhi, India.

Klingeman, P. C., Kehe, S. M., and Owusu, Y. A. (1984). "Streambank erosion protection and channel scour manipulation using rockfill dikes and gabions." *WRRI-98*, Oregon State University, Water Resources Research Institute, Corvallis, Oregon.

Komura, S. (1966). "Equilibrium depth of scour in long constrictions." *Journal of Hydraulic Engineering, ASCE*, 92(HY5), pp. 17-37.

Krebs, M., Zanke, U., and Mewis, P. (1999). "Hydro-morphodynamic modelling of groin fields." *28th IAHR congress*, Graz, Austria.

Kuhnle, R. A., Alvonso, C. V., and Shields, F. D. J. (1999). "Geometry of scour holes associated with 90° spur dikes." *Journal of Hydraulic Engineering, ASCE*, 125(9).

Noshi, H. M. (1997). "Abutment scour in uniform and stratified bed," PhD., Colorado State University, Fort Collins, Colorado, USA.

Ouillon, S., and Dartus, D. (1997). "Three-dimensional computation of flow around groyne." *Journal of Hydraulic Engineering, ASCE*, 123(11), pp. 962-970.

Peng, J., Kawahara, Y., and Tamai, N. (1997). "Numerical analysis of three-dimensional turbulent flows around submerged groynes." *27th IAHR congress,*, San Francisco, USA.

Peng, J., Tamai, N., Kawahara, Y., and Huang, G. W. (1999). "Numerical modelling of local scour around spur dikes." *28th IAHR congress*, Graz, Austria.

Przedwojski, B. (1995). "Bed topography and local scour in rivers with banks protected by groynes." *Journal of Hydraulic Research*, 33(2), pp. 257-273.

Przedwojski, B., Blazejewski, R., and Pilarczyk, K. W. (1995). *River training techniques-fundamentals, design and application*, A.A. Balkema, Rotterdam.

Rajaratnam, N. (1983). "Flow near groin-like structures." *Journal of Hydraulic Engineering, ASCE*, 109(3), 463-480.

Richardson, E. V., Stevens, M. A., and Simons, D. B. (1975). "The design of spurs for river training." *XVIth , IAHR congress*, Sao Paulo, Brazil, 382-388.

Schans, H. (1998). "Representativitet van kribvakmetingen uit 1996 en 1997 ten opzichte van de hele waal." *ICG 98/15*, Universieit Utrecht, Fysische Geografie, Utrecht.

Sieben, J., and Douben, N. (2000). "Globale inschatting van morfologische effecten in het zomerbed door herinrichting van uiterwaarden." *2000.027X*, RIZA, Arnhem.

Spannring, M. (1999). "Degradation of the river bed after building of groynes." *28th IAHR congress*, Graz, Austria.

Suzuki, K., Michiue, M., and Hinokidani, O. (1987). "Local bed form around a series of spur dikes in alluvial channels." *XXII IAHR Congress*, Lausanne, Belgium, 316-321.

Termes, A. P. P., van der Wal, M., and Verheij, H. J. (1991). "Waterbeweging door scheepvaart op rivieren en in kribvakken." *Q1046*, WL|Delft Hydraulics, Delft.

Tingsanchali, T., and Maheswarn, S. (1990). "2-d depth averaged flow computation near groyne." *Journal of Hydraulic Engineering, ASCE*, 116(1), pp. 71-85.

Tominaga, A., Ijima, K., and Nakano, Y. (2001). "Flow structures around submerged spur dikes with verious relative height." *29th IAHR CONGRESS*, Beijing, China, 421427.

Uijttewaal, W. S. J. (1999). "Groyne field velocity patterns determined with particle tracking velocimetry." *28th IAHR congress*, Graz, Austria.

Uijttewaal, W. S. J., Lehmann, D., and van Mazijk, A. (2001). "Exchange process between a river and its groyne fields - model experiments." *Journal of hydraulic Engineering, ASCE*, 127(11), pp. 928-936.

van Urk, G., and Smit, H. (1989). "The lower rhine geomorphological changes." Historical changes of large alluvial rivers: Western europe, G. E. Pettes, ed., John Wiley & Sons. Ltd, 167-182.

Verheij, H. J. (1997). "Effectiviteit van kribben." *Q2360*, WL|Delft Hydraulics, Delft.

Verheij, H. J., and van der Wal, M. (1984). "Prototype tests with respect to the stability of bank protection with various types of ships in the hartel canal in 1983 (text in dutch)." *M 1115*, WL | Delft Hydraulics, Delft.

Visser, P. J. (2000). "Bodemontwikkeling rijnsysteem." Delt University of Technology, Hydraulic and Offshore Engineering Section, Delft.

de Vriend, H. J. (1999). "Long-term morphodynamics of alluvial rivers and coasts." Environmental applications of mechanics and computer science, cism courses and lectures, G. Bianchi, ed., Springer Wien, New York, 1-19.

de Vries, M. (1996). "River engineering." *f10*, Delft University of Technology, Delft.

Wang, T. W., and Yanapirut, N. (1988). "Channel bed degradation caused by constriction." *6th Congress, Asian and Pacific Regional Division, IAHR*, Kyoto, Japan, 285-292.

WL|Delft_Hydraulics. (1987). “Kribvakerosie door zes- en vierbaksduwvaart op de waal.” *Q 93/Q 576*, WL | Delft Hydraulics, Delft.

APPENDIX I – CONCEPTUAL MODEL

Description

Groynes are constructed to provide a fixed river planform and a navigation channel that is relatively deep over a large part of its cross section. The success of the groynes in fulfilling they function depends on the balance of the hydrodynamic forces acting on the sandy deposits in the groyne-fields. This balance could be defined by the balance between erosion of sand that occurs due to currents and waves induced by navigation traffic, and deposition that probably takes place during times of high river discharge. As long as the erosion and deposition are in equilibrium on a time-scale of a couple of years, the groyne-fields are in a dynamic equilibrium, (ten Brinke et al., 1999)

To have an insight into the interaction between the morphology of the main channel of a river and that of the groyne-fields, we will assume that erosion of sediment from the groyne-fields occurs primarily due to navigation induced water motion, during times of normal to low river discharge. Whereas, the effect of navigation vanishes during times of high discharges, (WL|Delft_Hydraulics, 1987). Moreover, deposition of sand will take-place during times of high discharges with a rate that is a function of the discharge.

Figure I-1 is a schematic illustration for the basic assumption. Erosion takes place during a ship passage; deposition takes place at the times where there is no shipping with a much lower rate. The combined effect could be simplified by a straight line. The three line drawn for three different discharges $Q_1<Q_2<Q_3$. With the current state of knowledge, a more detailed "complex" function for the combined effect of navigation and discharge is not possible; more effort will be spent to define this relation through the course of the research.

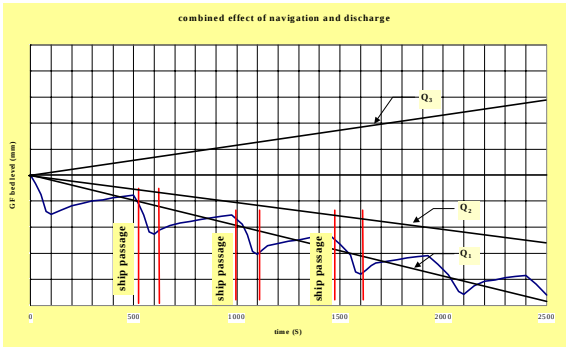

Figure I-1 Combined effect of navigation and discharge for three different discharges $Q_1<Q_2<Q_3$

For every discharge, we can estimate the sediment transport rate from the slope of line. Then, the relation between the discharge Q [m^3/s] and the sediment flux (S) [m^2/s] between the main channel and the groyne-fields could be deduced. We will assume again that this relation takes the form of a straight-line (Figure I-2). $S = a \cdot Q + b$

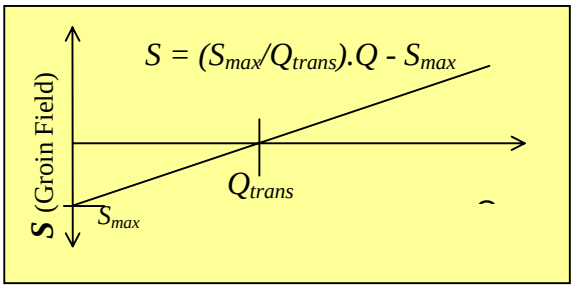

Figure I-2 S-Q Relation

Where:

S: sediment flux from the GF to MC per meter length of the GF-MC interfacial line [m^2/s]
a: constant = S_{max}/Q_{trans}
b: constant = $-S_{max}$
S_{max}*: maximum sediment flux from the GF to MC*
Q_{trans}*: the discharge at which the sediment flux changes direction*

The values of (a) and (b) could be chosen based on imperial values for (S_{max}) and (Q_{trans}), that could be obtained from field data and/or numerical computations. This relation is a simplified way of introducing the effect of both navigation and high river-discharge. The effect of navigation is assumed to be eroding the groyne-field at low to normal river-discharge, and will vanish during high river-discharge. The navigation effect will determine the value of (S_{max}). During the time that there is no navigation, some of the sediment that is transported to the main channel will be restored

to the groyne-fields, with a rate that is determined by the discharge value. The effect of discharge will determine the slope of the line. The compound effect of navigation and river discharge will determine the value of the transition discharge (Q_{trans}).

Application

Utilising the dimensions of the Waal River i.e. mean channel width of 250m, and mean groyne-field width of 60m, and applying the mass balance concept to a unit length of the river, with no supply or losses to the system. With the aid of the river discharge data (figure I-3), the morphological behaviour of the main channel and the groyne-field only due to their interaction could be obtained, (Figure I-4).

The value used for S_{max} were estimated from the field measurements results, performed by ten Brinke et al. (1999), who estimated a sediment flux from the groyne-fields to the main channel of 4.5 Kg/s for 15% of the time, with a dry density of 1500 Kg/m^3. This would be equivalent to a uniform sediment flux along the whole time of 2.25*10^{-6} m^2/s. The transition discharge were assumed to be 1450 m^3/s and the sediment porosity 40%.

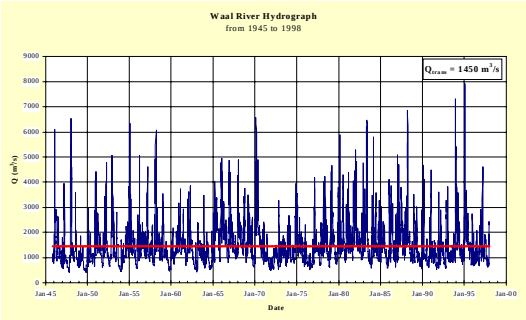

Figure I-3 Waal River discharge from 1945 to 1998

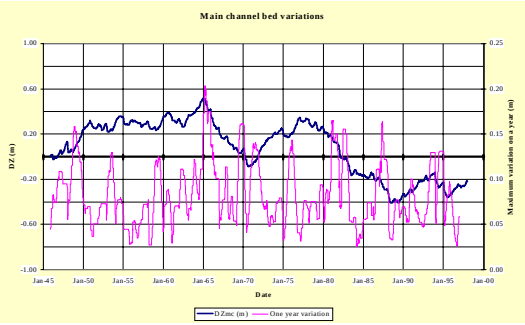

Figure I-4 Bed variations for the period from 1945 to 1998

Discussion

The results of this simple approach showed the dynamics of the interaction between the main channel and the groyne-fields. Provided that the channel bed level was in equilibrium at the beginning of the time series, The range of the channel bed variations was found to be in the order of ±0.50m for the whole time series (50 years). The variation over a year was found to have a maximum value of 0.20m, (Figure I-4).

By calculating the water level equivalent to each river discharge, the effect of the bed variations on the water level could be estimated. (Figure I-5) shows the percentage of water level increase/decrease due to the interaction between the groyne-fields and the main channel. It is obvious that the computed water level could vary by ±17.5% just because of the interaction between the groyne-fields and the main channel.

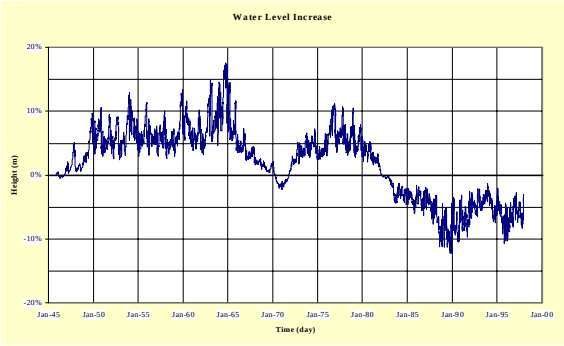

Figure I-5 Increase in water level due to the interaction between the *MC* and the *GF*

The discharge history of the river defines the starting point of the bed level computation for the next time step. Again, as there is no equilibrium bed levels that could be reached after a given period (morphological time scale),

the effect of the discharge history is very significant. On the one hand, a flood will have a much higher level if it is preceded by a long period of low discharges since the channel bed would have had a long period of aggregation as a consequence of the low discharges. On the other hand, a flood preceded by a flood will have a relatively lower water level as the channel would experience some degradation as a result of the earlier flood.

Through the analysis, the effect of both S_{max} and Q_{trans} were analysed. Changing the value of S_{max} changes the values of the bed variations with 1:1 proportion, but the shape and the transition points remains the same. Yet, changing the value of Q_{trans} would change the whole pattern of the channel bed variations leading to changes in the bed level with a much higher magnitude.

Conclusions

This conceptual model succeeded to show the dynamics of the interaction between the groyne-fields and the main channel. However, it requires improvement.

The values of channel bed variations, (aggregation/degradation) might be over-estimated with this approach. Moreover, the bed variations could reach $\pm\infty$, which is not possible in reality. This is due to the fact that in this simple approach there is no slow-down mechanism that could control the morphological process i.e. equilibrium bed level(s).

The effect of discharge history in this approach is very significant. The absence of an equilibrium bed level or as consequence to that, the absence of a morphological time-scale effect allows the effect of the discharge history to extend over a very long period (infinite in this model).

The choice of the S_{max} might be easy and straightforward as it only affects the values of the bed variations. Nevertheless, the choice of a value for Q_{trans} might change the pattern of the bed variations so it is very important to make an accurate choice for Q_{trans}.

Recommendations

It is very important to define two different equilibrium bed levels for the groyne-fields. The first is the groyne-field's minimum bed level, after which the navigation-induced erosion would vanish. The second is the groyne-field's maximum bed level, after which the sedimentation due to high discharge would stop.

The morphological time-scale associated with the groyne-fields, main channel interaction is a factor that plays an important role on the extent of the effect of the discharge history, i.e. the influence of that interaction on the flood levels.

APPENDIX II – THE MODEL OF SIEBEN & DOUBEN

The aim of this simplified model is to have a theoretical understanding for the morphological behaviour of the groyne-fields. A very important limitation for this model, that it is limited to the low-water condition, i.e. the groynes are not submerged.

Mass Balance

With reference to the definition sketch the groyne-field (GF) bed level is in balance with the vertical sediment flux (F), and the sediment balance reads:

$$(1-\varepsilon)\cdot A_{gf}\cdot\frac{\partial z_{gf}}{\partial t}+F=D-E \qquad \text{(II.1)}$$

Where:

A_{gf} = L_{gf} x L_g [m^2]
ε = porosity [--]

With the vertical sediment flux (F) as

$$F=w`\cdot A_{gf}\cdot(c_e-c) \qquad \text{(II.2)}$$

Where:

w‘ = exchange rate between GF bed material, and water [m/s]
C_e = equilibrium concentration in the GF
C = actual concentration in the GF

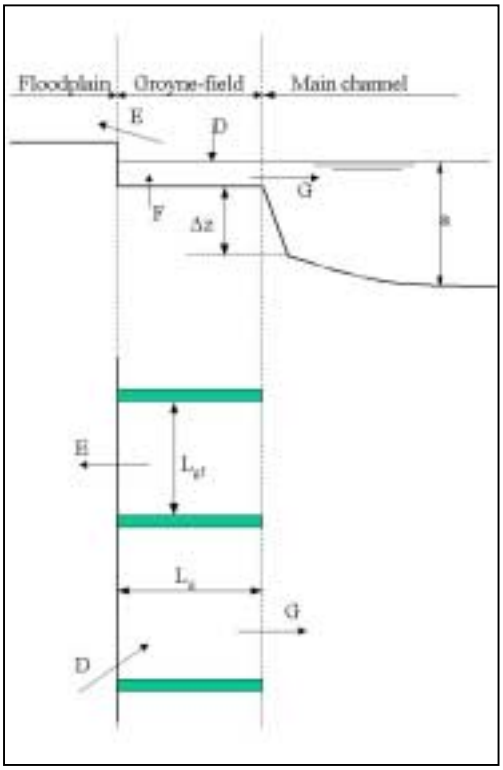

Figure II-1 Definition sketch for a river with groynes, after Sieben & Douben (2000)

Sediment concentration

Both the equilibrium, and the actual concentration is not easy to define or estimate for the complex flow in a groyne-field, but for simplicity we may assume that:

$$C_e=C_{re}\cdot\theta_{gf}^{b/2}$$

$$C=e^{-k\cdot\frac{\Delta z}{a}}\cdot\chi\cdot\frac{q_s}{q} \qquad \text{(II.3)}$$

Where:

C = actual concentration in the GF
θ_{gf} = effective GF dimensionless shear stress (Shields parameter) [-]
C_{re} = reference concentration in the main channel
b = empirical factor
K = damping factor (for the concentration over the depth)
χ = steering factor (relates the concentration in GF to the one the main channel)
q = specific discharge [m^2/s]
q_s = specific sediment load in the main channel [m^2/s]

The values for both parameters (C_{re}), and (b) must be analysed from the prototype data. For the estimation of the steering factor (χ) along the Waal River, (Lenders et al., 1998 – after Sieben & Douben, 2000) showed that a base sediment concentration in the GF (flow induced) $C_{flow} = 2*10^{-5}$, and a peak concentration (navigation induced) $C_{nav} = 2*10^{-4}$, i.e. $C_{nav} = 10*C_{flow}$.

Assuming that the average ship passing time is around 100s, and an average frequency of about one ship every three minutes, i.e. the percentage of time that there is a ship passing (p) ≅ 0.50. Consequently, the time of high concentration (C_{nav}) could be estimated to take place for around 50% of the time, and a rough estimate for $\chi \cong 6$, is possible.

In addition to the navigation-induced disturbances, there is another effect for the relative depth $(\frac{\Delta z}{a})$ of the groyne-field; (this effect will not be included in this model)

Effective shear stress in the groyne-field

Two different conditions should be distinguished for the estimation of effective shear stress in a groyne-field. The first is the normal flow condition in the absence of any navigation effect, and the second is the combined flow with navigation-induced water motion.

For the case of normal flow only, we may assume that the flow velocity in a groyne-field is proportional to that in the main channel with a factor $\alpha \cong 0.1$ to 0.4, this factor could be estimated from prototype measurements, laboratory experiments or at least from numerical simulations.

For the situation of navigation-induced water motion, based on the experiments that were done by WL|Delft_Hydraulics (1987), the outflow from a groyne-field could be averaged along the ship passage time, in the following way:

$$Q_{out} = \frac{\Delta h \cdot L_g \cdot L_{gf}}{T_{passage}} \tag{II.4}$$

Where:

Q_{out} = exchange flow rate between the groyne-field and the main channel [m^3/s]
Δh = water level depression caused by a ship passage [m]
$T_{passage}$ = average ship passage time [s]

Typical values for the water level depression $\Delta h \cong 0.2$~0.5m, and for the passage time $T_{passage} \cong$ 100s.

The outflow velocity u_{out} could as well, be written in the following form,

$$u_{out} = \frac{\Delta h}{T_{passage}} \cdot \frac{L_g}{a - \Delta z} \tag{II.5}$$

Assuming a linear relation between the dimensionless shear stress in the groyne-field (θ_{gf}) and the main channel (θ) i.e.

$$\theta_{gf} = f \cdot \theta; \qquad \theta = \frac{u_{mc}^2}{C_h \cdot \Delta \cdot D_{50}}; \qquad f = \alpha^2 \left[p \cdot (\frac{u_{out}}{\alpha \cdot u_{mc}})^2 + 1 \right] \tag{II.6}$$

Where:

C_h = Chezy coefficient for the main channel [$m^{½}/s$]
Δ = sediment specific weight [-]
f = proportionality factor [-]
p = percentage of time that there is a ship passing [-]

A typical value for (f) is 0.03 for the conditions of the Waal River

Equilibrium bed level

For the groyne-field bed level equilibrium to occur, the sediment flux (F) should vanish i.e. ($F \rightarrow 0$), which means that $C = C_e$, then the definition of the bed variations could be written as:

$$e^{-k(\frac{\Delta z}{a})} \cdot \chi \cdot \frac{q_s}{q} = C_{re} \cdot f \cdot \theta^{b/2} \qquad \text{(II.7)}$$

We must realise that it is a dynamic equilibrium, which could be explained in the following way. The navigation-induced water motion creates a higher sediment concentration inside the groyne-field, while the concentration in the main channel (q_s/q) is almost constant. The damping factor represented in the left-hand side of the equation [$-k \cdot(\Delta z/a)$] must increase, by taking a lower value for the groyne-field bed level (Δz), (EROSION). On the other hand, in the absence of navigation, the damping factors must decrease through a higher value for (Δz), (SEDIMENTATION).

An expression for (q_s/q) could be estimated with a combination between Engelund & Hansen sediment transport formula, and Chezy equation,

$$\frac{q_s}{q} = X \cdot \theta^{(n-3)/2}; \qquad where\ X = \frac{0.084 \cdot i}{\Delta} \cdot \frac{C_h}{\sqrt{g}} \qquad [-]$$

Finally, the equilibrium bed level could be written in the following form;

$$\frac{\Delta z}{a} = A + B \cdot \ln \theta \qquad \text{(II.8)}$$

Where:

$$A = \ln\left(\frac{C_{re} \cdot f^{b/2}}{\chi \cdot X} \right)^{-1/k}$$

$$B = \frac{b - n + 3}{-2k}$$

<u>Time-scale for groyne-field bed variations</u>

Without any sediment supply to the groyne-field ($D = 0$), and no sediment outflow to the floodplain ($E = 0$), the mass balance could be written in the following form,

$$(1-\varepsilon)\frac{\partial z}{\partial t} + w`\cdot(C_{re} \cdot \theta^{b/2} - e^{-k(\frac{\Delta z}{a})} \cdot \chi \frac{q_s}{q}) = 0 \qquad \text{(II.9)}$$

and, if

$$\frac{\Delta z}{a} = \frac{\Delta z_e}{a} + \frac{\Delta z`}{a}$$

then, we can rewrite;

$$(1-\varepsilon)\frac{\partial(\Delta z`)}{\partial t} + w`\cdot(C_{re} \cdot \theta^{b/2} - e^{-k(\frac{\Delta z_e}{a} + \frac{\Delta z`}{a})} \cdot \chi \frac{q_s}{q}) = 0 \qquad \text{(II.10)}$$

Utilising Taylor expansion the following expression could be reached;

$$\frac{\partial(\Delta z`/a)}{\partial t} + \frac{\Delta z`/a}{T_m} = 0$$

$$T_m = \frac{a}{k \cdot w`} \cdot \frac{(1-\varepsilon)}{\chi \cdot (\frac{q_s}{q})} \qquad \text{(II.11)}$$

Where, T_m [s], is the morphological time-scale for the groyne-field bed variations. Sieben, (2000) estimated the morphological time-scale for the groyne-fields bed variations for the Waal River conditions, to be around 50 days.

Sediment Exchange

Using the above-described model, Figure II-1, the sediment exchange between the groyne-field and the main channel could be roughly estimated. The mass balance could be written the following way:

$$A_{gf} \cdot \frac{\partial c\,(a-\Delta z)}{\partial t} - F + G \cdot L_{gf} = 0 \qquad \text{(II.12)}$$

For the value of the horizontal flux (G) to be determined, the time variation of the suspended sediment "1st term of the equation", and the vertical flux (F) must be first defined. The vertical flux is defined in equation (I.2), the horizontal flux could then be written;

$$G \cdot L_{gf} = -A_{gf} \cdot (a-\Delta z)\frac{\partial c}{\partial t} - A_{gf} \cdot c\frac{\partial (a-\Delta z)}{\partial t} + w` \cdot A_{gf} \cdot (c_e - c) \qquad \text{(II.13)}$$

For c>>1.0, then:

$$G \cong -L_{gf} \cdot (1-\varepsilon)\frac{\partial z_{gf}}{\partial t} + \frac{D-E}{L_{gf}} \qquad \text{(II.14)}$$

The sediment balance in the main channel could be now written;

$$B_{mc}\frac{\partial z_{mc}}{\partial t} + \frac{\partial B\,q_s}{\partial x} = \frac{G}{(1-\varepsilon)} - \frac{V_{\text{dredging}}}{(1\text{-}\varepsilon)} \qquad \text{(II.15)}$$

for c<<1, we can use equation (I.14) to substitute for (G), then:

$$B_{mc}\frac{\partial z_{mc}}{\partial t} + \frac{\partial B\,q_s}{\partial x} = -L_{gf}\frac{\partial z_{gf}}{\partial t} + \frac{D-E}{L_{gf} \cdot (1-\varepsilon)} \qquad \text{(II.16)}$$

For the basic equation, de Vries (1996) showed that it could be simplified to:

i- *Simple-wave model* – for small-scale morphological changes,

$$\frac{\partial z}{\partial t} + \frac{c_0}{\alpha_0} \cdot \frac{\partial z}{\partial x} = 0$$

with, $$\frac{c_0}{\alpha_0} = \frac{1}{1-F_r^2} \cdot \left(\frac{dq_s}{du} \cdot \frac{u_0}{a}\right)$$

then, $$\frac{\partial z}{\partial t} + \frac{n\,q_s}{a\,(1-F_r^{\,2})} \cdot \frac{\partial z}{\partial x} = 0$$

ii- *Parabolic model* – for large-scale morphological changes,

$$\frac{\partial z}{\partial t} - K_0 \cdot \frac{\partial^2 z}{\partial x^2} = 0$$

with, $$K_0 = \frac{c_0}{A_0} = \frac{1}{\left(\frac{3i}{a}\right)} \cdot \left(\frac{dq_s}{du} \cdot \frac{u_0}{a}\right)$$

then, $$\frac{\partial z}{\partial t} - \frac{n\,q_s}{3i} \cdot \frac{\partial^2 z}{\partial x^2} = 0$$

Applying the same concept to equation (1.16), we end up with two equations describing the main channel bed variations due to the interaction with the groyne-fields. Neglecting any losses 'dredging', or supply 'filling' to the system, the two equations will take the following form:

$$\left[1-\frac{c\,k}{(1-\varepsilon)}\frac{L_g}{B_{mc}}k\,(1-\frac{\Delta z}{a})^2\right]\cdot\frac{\partial z_{mc}}{\partial t}+\frac{u}{a}\frac{dq_s}{du}\cdot\frac{\partial z_{mc}}{\partial x}=\left[\frac{L_g}{B_{mc}}\frac{1}{(1-\varepsilon)}\left(c-c\,k(1-\frac{\Delta z}{a})-1+\varepsilon\right)\right]\cdot\frac{\partial z_{gf}}{\partial t}$$

Simple-wave model (II.17)

$$\left[1-\frac{c\,k}{(1-\varepsilon)}\frac{L_g}{B_{mc}}k\,(1-\frac{\Delta z}{a})^2\right]\cdot\frac{\partial z_{mc}}{\partial t}+\frac{u}{3i}\frac{dq_s}{du}\cdot\frac{\partial^2 z_{mc}}{\partial x^2}=\left[\frac{L_g}{B_{mc}}\frac{1}{(1-\varepsilon)}\left(c-c\,k(1-\frac{\Delta z}{a})-1+\varepsilon\right)\right]\cdot\frac{\partial z_{gf}}{\partial t}$$

Parabolic model (II.18)